Bifunctional Covalent Organic Frameworks with Two Dimensional Organocatalytic Micropores

Digambar Balaji Shinde,[a,‡] Sharath Kandambeth,[a,‡] Pradip Pachfule,[a] Raya Rahul Kumar,[a] and Rahul Banerjee[a]*

[a]Physical/Materials Chemistry Division, CSIR- National Chemical Laboratory, Dr. Homi Bhabha Road, Pune 411008, India.

Supporting Information

Section	Name	Page No
S-1	**General Information**	**2**
S-2	**Synthetic Procedures**	**2**
S-3	**Structural Modeling and Atomic Coordinates of COFs.**	**4**
S-4	**Powder X-Ray Diffraction Analysis (PXRD)**	**8**
S-5	**FT-IR Spectra**	**11**
S-6	**^{13}C CP/MAS NMR Spectra**	**12**
S-7	**^{1}H and ^{13}C NMR Spectra of reference compound**	**13**
S-8	**Gas Adsorption Studies of 2,3-DhaTph and 2,3-DmaTph**	**15**
S-9	**Thermo Gravimetric Analysis (TGA)**	**20**
S-10	**Scanning Electron Microscopy (SEM) and Transmission Electron Micrograph (TEM)**	**21**
S-11	**X-Ray investigation of single crystals of linker-2,3-DhaTph and 2,3-DmaTph**	**22**
S-12	**Stability test for 2,3-DhaTph and 2,3-DmaTph**	**23**
S-13	**Before and after Catalyst (2,3-DhaTph and 2,3-DmaTph)**	**28**
S-14	**Optimization of catalyst**	**31**
S-15	**Reference**	**33**

Section S-1: General Information

***General Remarks*:** 2,3-dimethoxyterephthalaldehyde (2,3-**Dma**) or 2,3-dihydroxyterephthalaldehyde (2,3-**Dha**) was synthesized by 1,2-dimethoxybenzene[1]. All other reagents and solvents were commercially available and used as received. Powder X-ray diffraction (PXRD) patterns were recorded on a Phillips PANalyticaldiffractometer for Cu K_α radiation (λ = 1.5406 Å), with a scan speed of 1° min^{-1} and a step size of 0.02° in 2θ. Fourier transform infrared (FT-IR) spectra were taken on a Bruker Optics ALPHA-E spectrometer with a universal Zn-Se ATR (attenuated total reflection) accessory in the 600-4000 cm^{-1} region or using a Diamond ATR (Golden Gate). Thermo gravimetric analyses (TGA) were carried out on a TG50 analyzer (Mettler-Toledo) or a SDT Q600 TG-DTA analyzer under N_2 atmosphere at a heating rate of 10 ºC min^{-1} within a temperature range of 30-900 °C. SEM images were obtained with a Zeiss DSM 950 scanning electron microscope and FEI, QUANTA 200 3D Scanning Electron Microscope with tungsten filament as electron source operated at 10 kV. The samples were sputtered with Au (nano-sized film) prior to imaging by a SCD 040 Balzers Union. TEM images were recorded using FEI Tecnai G2 F20 X-TWIN TEM at an accelerating voltage of 200 kV.The TEM Samples were prepared by dropcasting the sample from isopropanol on copper grids TEM Window (TED PELLA, INC. 200 mesh).All gas adsorption experiments (up to 1 bar) were performed on a *Quantachrome Quadrasorb* automatic volumetric instrument. Solid state NMR (SSNMR) and ligand NMR was taken in a Bruker 300 MHz NMR spectrometer.

Section S-2: Synthetic procedures

2,3-DhaTph: The synthesis of **2,3-DhaTph** was carried out by utilizing the same protocol with a mixture of 2,3-dihydroxyterephthalaldehyde (**2,3-Dha**) (26.6 mg, 0.16 mmol) and tetra(*p*-amino-phenyl)porphyrin (**Tph**) (54 mg, 0.08 mmol) in presence of 6.0 M acetic acid (0.6 mL) using 1,2-dichlorobenzene (o-DCB) (1.0 mL) and dimethyl acetamide (DMAc) (3.0 mL). This mixture was sonicated for 20 minutes in order to get a homogenous dispersion. The tube was then flash frozen at 77 K (liquid N_2 bath) and degassed by three freeze-pump-thaw cycles. The tube was sealed off and then heated at 120 °C for 72 hours. After the reaction the COF powders are filtered out, washed with ethanol and dried under vacuum at 150 °C for 12 hours to give purple colored powder in 80 % (56 mg) isolated yield based on **Tph**. **IR (powder): υmax** 1612, 1547, 1471, 1352, 1301, 1205, 965, 856, 793, 729 cm^{-1}.

Elemental Analysis data: Anal. Calcld. For $C_{60}O_4N_8H_{38}$.2H2O: C, 74.21; H, 4.36; N, 11.54; found: C, 73.42; H, 4.21; N, 11.37.

3,6-bis((*E*)-(phenylimino)methyl)benzene-1,2-diol (Reference compound for 2,3-DhaTph): The reference compound was synthesized by the reaction between 2,5-dihydroxyterephthalaldehyde (**2,3-Dha**) (83 mg, 0.5 mmol) and aniline (113 mg, 1.25 mmol) in 30 mL ethanol under refluxing condition for 24 h. After this time the solution was cooled to room temperature and the precipitate was collected by filtration, washed with ethanol, and dried under vacuum to give 129 mg, 82% of a yellow solid. **FT-IR (powder): υmax** 1614, 1588, 1510, 1459, 1399, 1333, 1287, 1245, 1193, 1152, 872, 795, 762 cm^{-1}; **^{1}H NMR** (1,1,2,2-Tetrachloroethane-d_2, 400 MHz): δ 13.06 (2H, s), 8.03 (2H, s), 6.84 (4H, t, *J* = 7.78 Hz), 6.73-6.70 (6H, m), 6.41 (2H, s); **^{13}C NMR** (1,2,2-Tetrachloroethane-d_2, 100 MHz): δ 161.3, 150.2, 147.4, 128.9, 126.9, 120.7, 120.6, and 120.1.

2,3-DmaTph: The synthesis of 2,3-**DmaTph** was carried out by utilizing the same protocol with a mixture of 2,3-dimethoxyterephthalaldehyde (2,3-**Dma**) (31.0 mg, 0.16 mmol) and tetra(*p*-amino-phenyl)porphyrin (**Tph**) (54.0 mg, 0.08 mmol) in presence of 6.0 M acetic acid (0.4 mL) using 1,2-dichlorobenzene (o-DCB) (1.0 mL) and dimethyl acetamide (DMAc) (3.0 mL). This mixture was sonicated for 20 minutes in order to get a homogenous dispersion. The tube was then flash frozen at 77 K (liquid N_2 bath) and degassed by three freeze-pump-thaw cycles. The tube was sealed off and then heated at 120 °C for 72 hours. After the reaction the COF powders are filtered out, washed with ethanol and dried under vacuum at 150 °C for 12 hours to give purple colored powder in 74 % (52 mg) isolated yield based on **Tph**. **IR (powder): υmax** 1608,1509, 1474, 1399, 1305, 963, 854, 796, 725 cm^{-1}. **Elemental Analysis data**: Anal. Calcld. For $C_{64}O_4N_8H_{46}$.2H2O: C, 74.84; H, 4.91; N, 10.91; found: C, 73.87; H, 4.51; N, 11.79.

(*1E,1'E*)-1,1'-(2,3-dimethoxy-1,4-phenylene)bis(*N*-phenylmethanimine) (Reference compound for 2,3-DmaTph): The reference compound was synthesized by the reaction between 2,3-dimethoxyterephthalaldehyde (**2,3-Dma**) (97 mg, 0.5 mmol) and aniline (113 mg, 1.25 mmol) in 20 mL ethanol under refluxing condition for 24 h. After this time the solution was cooled to room temperature and the precipitate was collected by filtration, washed with ethanol, and dried under vacuum to give 131 mg, 82 % of a yellow solid. **FT-IR (powder): υmax** 1616, 1586, 1561, 1453, 1408, 1361, 1263, 1203, 1166, 1051, 1013, 909, 864, 827, 756, 684cm^{-1}; **^{1}H NMR** ($CDCl_3$/CCl_4, 400 MHz): δ 8.71 (2H, d, *J* = 7.8 Hz), 7.92

(s, 2H), 7.31-7.29 (m, 4H), 7.15-7.13 (m, 6H), 3.90 (s, 6H); **^{13}C NMR** ($CDCl_3/CCl_4$, 100 MHz): δ 154.9, 153.9, 152.3, 132.8, 129.1, 126.2, 122.7, 121.1, and 61.8

Section S-3: Structure Modeling and Atomic Coordinates of COFs.

Atomic positions and cell sizes of modeled COF layers were optimized using Self-Consistent Charge Density Functional Tight-Binding (SCC-DFTB) Method. Stacking of layers are affected by the Coulomb repulsion between the partial atomic charges in adjacent layers. Hence, we performed Mulliken population analysis for the charges. The adjacent layers were shifted with respect to each other in different directions in order to avoid Coulomb repulsion from charges alike. Several possibilities were considered, however, the best was taken from comparison of simulated PXRD pattern with the experimental. Interlayer separation was also determined from the comparison of PXRD patterns. The fractional coordinates of **2,3-DhaTph** and **2,3-DmaTph** are given in **Table S1** and **Table S2** respectively.

Table S1. Fractional atomic coordinates for the unit cell of 2,3-DhaTph

2,3-DhaTph			
P-1 **a = 24.7, b = 24.6, Å, c = 4.0 Å** **α = 92.9°, β = 90.2°, γ = 92.7°**			
N1	0.56133	0.46819	1.59541
N2	0.44776	0.58163	1.46164
N3	0.448	0.46977	1.55723
N4	0.56109	0.58006	1.49982
C1	0.61356	0.47624	1.56792
C2	0.39553	0.57359	1.48913
C3	0.63876	0.42702	1.5557
C4	0.37033	0.6228	1.50135
C5	0.6006	0.38959	1.57223
C6	0.40849	0.66024	1.48481
C7	0.55217	0.4159	1.59443
C8	0.45692	0.63392	1.46262
C9	0.50354	0.39168	1.58914
C10	0.50555	0.65814	1.46791
C11	0.50147	0.33188	1.56735
C12	0.50687	0.72176	1.49377

C13	0.52472	0.30155	1.81269
C14	0.48393	0.74871	1.2443
C15	0.52543	0.24789	1.78493
C16	0.50258	0.22399	1.51413
C17	0.47879	0.25348	1.2695
C18	0.47856	0.30729	1.29416
C19	0.45605	0.41762	1.58459
C20	0.55304	0.6322	1.47246
C21	0.4071	0.39158	1.60773
C22	0.60199	0.65825	1.44932
C23	0.36937	0.42957	1.58876
C24	0.63972	0.62026	1.46829
C25	0.39573	0.47793	1.55601
C26	0.61336	0.57189	1.50104
C27	0.63863	0.52414	1.535
C28	0.37046	0.52569	1.52205
C29	0.31104	0.52607	1.52516
C30	0.72376	0.50452	1.8035
C31	0.28371	0.54524	1.25307
C32	0.77971	0.50417	1.80339
C33	0.22979	0.54569	1.25326
C34	0.20296	0.52593	1.51927
C35	0.78026	0.54349	1.2676
C36	0.22924	0.50637	1.78905
C37	0.28311	0.50684	1.79558
N5	0.86402	0.52886	1.52431
O1	0.95514	0.58745	1.51714
C38	0.89179	0.48822	1.56157
C39	0.80686	0.5235	1.52321
C40	0.9467	0.49109	1.53833
C41	0.96945	0.44084	1.53576
C42	0.97569	0.53877	1.50534
C43	0.69778	0.52277	1.54057
C44	0.7232	0.54301	1.27221
N6	0.14566	0.52865	1.49905
O2	0.05842	0.58255	1.41288

C45	0.11273	0.48771	1.51428
C46	0.05747	0.48732	1.49246
C47	0.02834	0.43969	1.53115
C48	0.03152	0.5357	1.46087
N7	0.50756	0.17193	1.50349
O3	0.56739	0.08347	1.52218
C49	0.46945	0.14357	1.52989
C50	0.47419	0.08221	1.51358
C51	0.42925	0.05375	1.53716
C52	0.52264	0.05721	1.53602
C53	0.48273	0.8025	1.25817
C54	0.5261	0.80069	1.78067
N8	0.50924	0.88151	1.54452
O4	0.56361	0.97008	1.55396
C55	0.46833	0.90933	1.52556
C56	0.50415	0.8284	1.53693
C57	0.4704	0.97047	1.55979
C58	0.42952	0.99928	1.54315
C59	0.52291	0.99581	1.5464
C60	0.52574	0.7457	1.76558

Table S2. Fractional atomic coordinates for the unit cell of 2,3-DmaTph

2,3-DmaTph			
***P*-1** **a = 25.2, b = 24.6, Å, c = 4.1 Å** **α = 90.1, β = 89.7, γ = 88.4**			
C1	0.30017	1.00815	0.79238
C2	0.27515	1.02662	1.07999
C3	0.22062	1.02493	1.10627
C4	0.46463	1.03426	0.58829
C5	0.19043	1.00577	0.84038
C6	0.13329	1.00457	0.86522
N1	0.35693	1.01037	0.77547
C7	0.21616	0.98857	0.54775
C8	0.27069	0.98942	0.52472

C9	0.386	0.97781	0.60928
C10	0.47702	0.9399	0.60796
C11	0.44337	0.98387	0.60704
N2	1.05689	0.94598	0.86502
C12	1.10892	0.95499	0.86853
C13	1.13691	0.90509	0.85792
C14	1.05025	0.89363	0.84935
C15	1.10139	0.86797	0.84124
C16	0.69583	0.99294	0.79387
C17	0.72159	0.98009	1.0912
C18	0.77611	0.98336	1.11284
C19	0.53188	0.9472	0.58359
C20	0.80558	0.99817	0.83269
C21	0.86354	0.99927	0.84735
N3	0.64022	0.98611	0.7759
C22	0.7799	1.01103	0.53431
C23	0.7254	1.00865	0.51536
C24	0.60915	1.00966	0.56769
C25	0.51848	1.04157	0.56831
C26	0.55256	0.99872	0.57153
N4	0.93987	1.05789	0.86436
C27	0.88789	1.04884	0.84896
C28	0.85986	1.09871	0.84324
C29	0.94649	1.11028	0.86679
C30	0.89536	1.13594	0.85208
C31	0.99104	1.30167	0.79647
C32	0.97498	1.2765	1.08934
C33	0.9767	1.22195	1.11305
C34	0.96473	0.46813	0.59111
C35	0.99331	1.19191	0.8397
C36	0.99494	1.13684	0.86374
N5	0.98896	1.36049	0.78135
C37	1.00777	1.21983	0.54187
C38	1.00712	1.27438	0.5215
C39	1.02092	1.38933	0.60888
C40	1.05916	1.48017	0.59955

C41	1.01508	1.4467	0.60557
N6	0.05423	1.06038	0.89738
C42	0.04462	1.11213	0.86348
C43	0.0917	1.13823	0.82323
C44	0.10636	1.05304	0.86456
C45	0.13038	1.10109	0.82047
C46	1.00831	0.7022	0.78324
C47	1.02606	0.72789	1.07042
C48	1.02285	0.78236	1.09611
C49	1.05203	1.53502	0.57222
C50	1.003	0.81192	0.82923
C51	1.00179	0.86708	0.84603
N7	1.01512	0.64378	0.76049
C52	0.98508	0.78345	0.54128
C53	0.98752	0.72898	0.51871
C54	0.9897	0.61253	0.5627
C55	0.95757	0.52196	0.56897
C56	1.00055	0.55589	0.56526
N8	0.9427	0.94369	0.8324
C57	0.95228	0.89187	0.85829
C58	0.90532	0.86557	0.89619
C59	0.89049	0.95085	0.85957
C60	0.86645	0.90257	0.89406
O1	0.56417	0.90277	0.5645
O2	0.45715	0.88878	0.63553
C61	0.61882	0.90396	0.50977
C62	0.40353	0.88595	0.73143
O3	1.09653	1.56705	0.54538
O4	1.11027	1.46009	0.62288
C63	1.09535	1.62265	0.48291
C64	1.11317	1.40531	0.71993

Section S-4: Powder X-Ray Diffraction Analysis (PXRD)

In order to elucidate the structure of these COFs and to calculate the unit cell parameters, possible 2-D models were optimized using Density Functional Tight-Binding method. Several stacking possibilities were considered for reasons reported in the literature.[2] The experimental PXRD patterns are agreeable with the simulated patterns of some near-eclipsed stacking models (Figure S1 and S2 in ESI). Hence we propose structures close to Tetragonal space group (*P1*) for 2,3-**DhaTph and 2,3-DmaTph** by comparing the experimental and simulated PXRD patterns. Refinements of PXRD pattern were done using Reflex module of Material studio.[3]

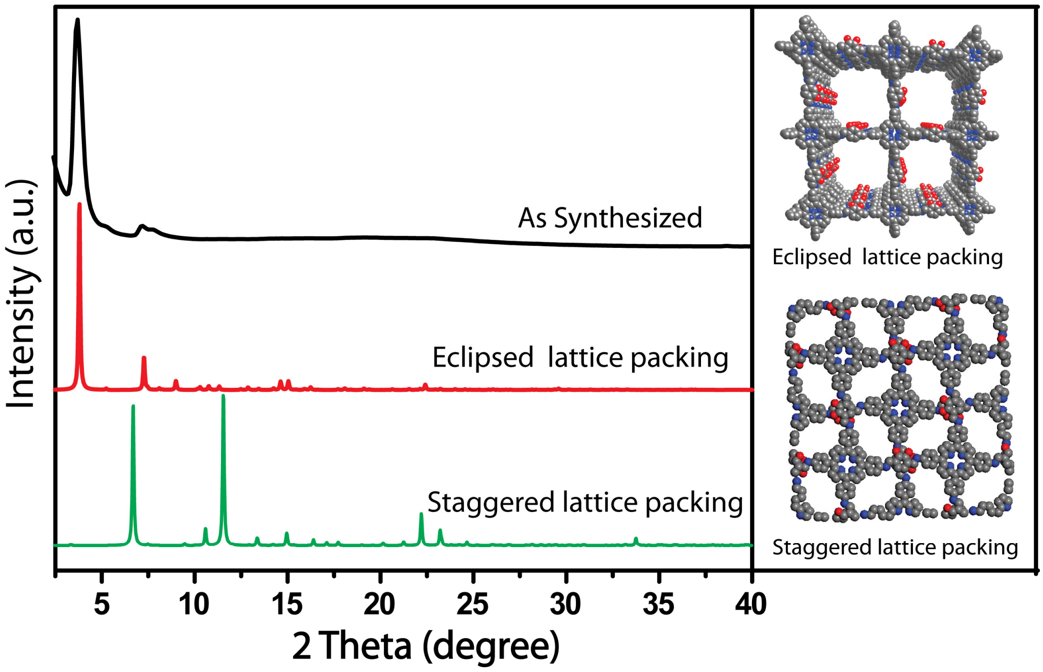

Figure S1: PXRD pattern of As-synthesized **2,3-DhaTph** (Black) compared with the eclipsed (Red) and staggered (Green) stacking models.

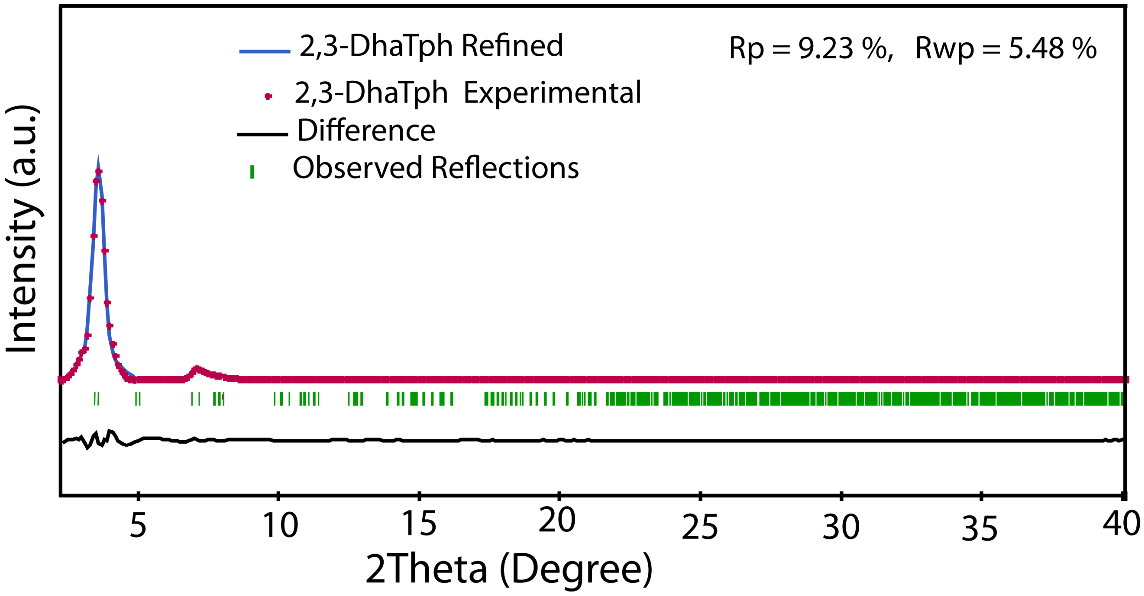

Figure S2: Experimental (Red) compared with refined (Blue) PXRD profiles of **2,3-DhaTph** with an eclipsed arrangement; Observed reflections (Green) and difference plot is given in (Black).

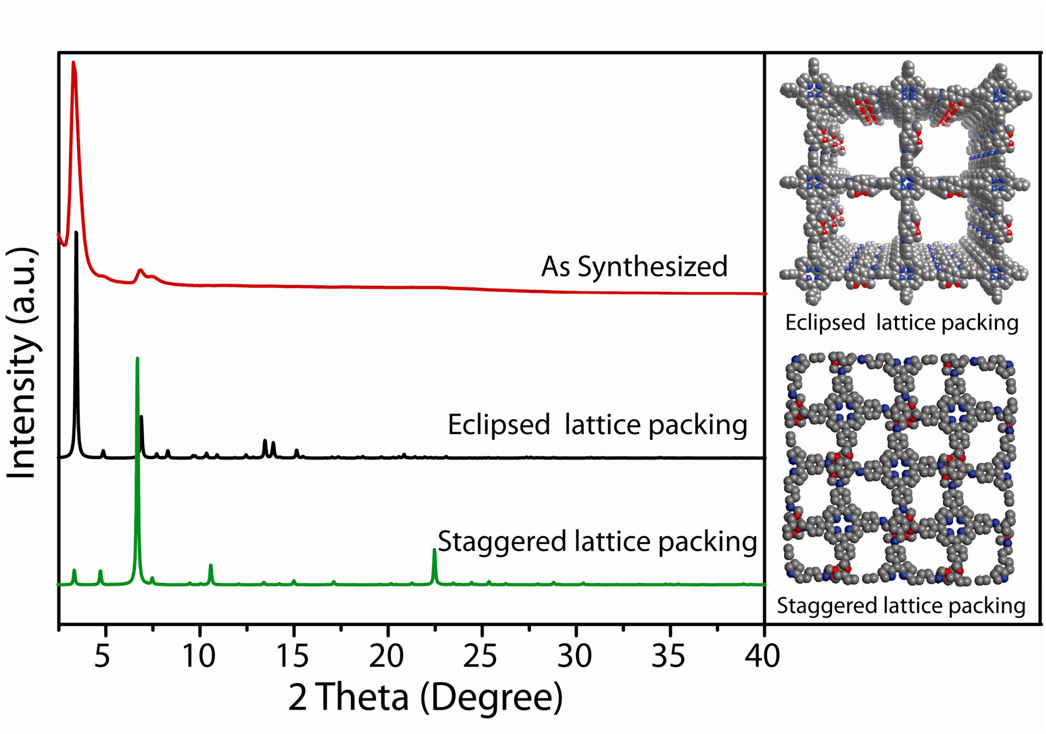

Figure S3: PXRD pattern of As-synthesized **2,3-DhaTph** (Black) compared with the eclipsed (Red) and staggered (Green) stacking models.

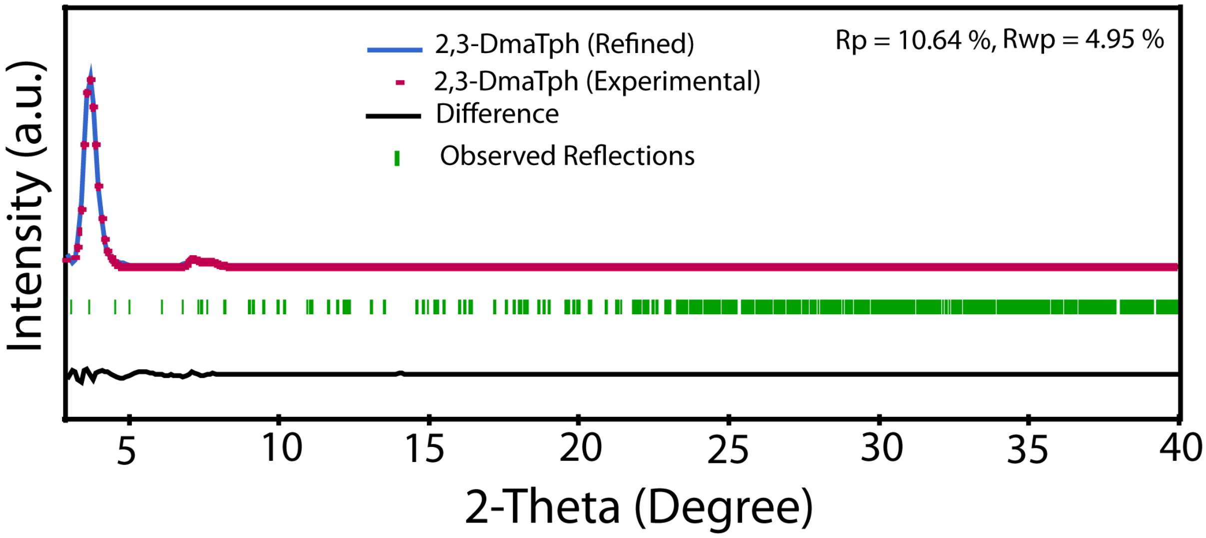

Figure S4: Experimental (Red) compared with refined (Blue) PXRD profiles of **2,3-DmaTph** with an eclipsed arrangement; Observed reflections (Green) and difference plot is given in (Black).

Section S-5: FT-IR Spectra

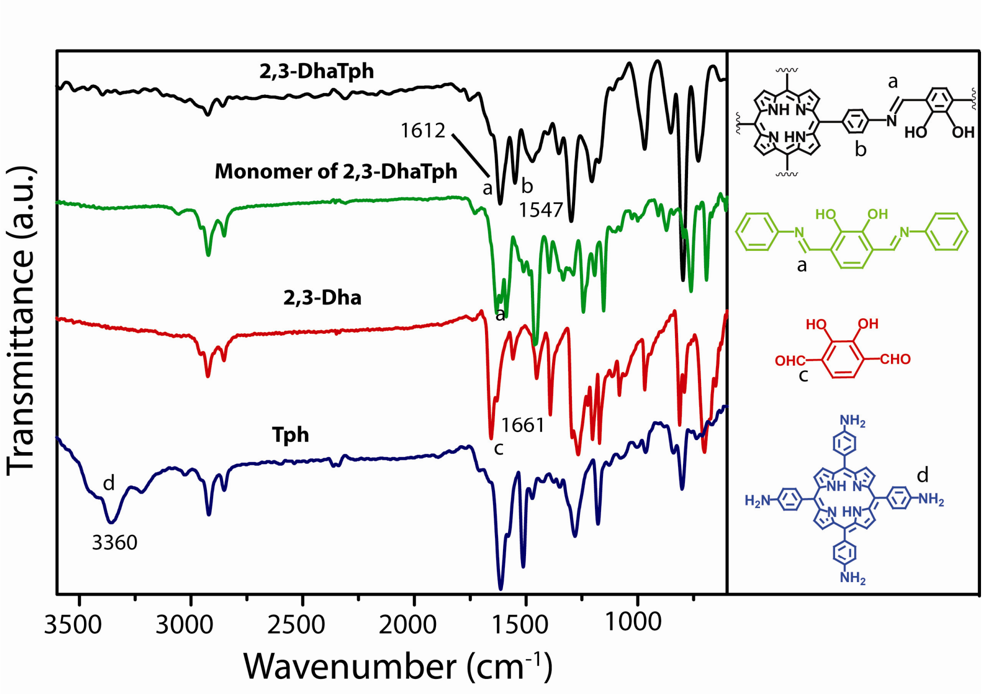

Figure S5: FT-IR spectra of **2,3-DhaTph** (Black), 3,6-bis((*E*)-(phenylimino)methyl)benzene-1,2-diol (Green) (Monomer of **2,3-DhaTph**), 2,3-dihydroxyterephthalaldehyde (2,3-**Dha**) (Red), and 5,10,15,20-Tetrakis-(4-aminophenyl)-21H,23H-porphine (**Tph**) (Blue).

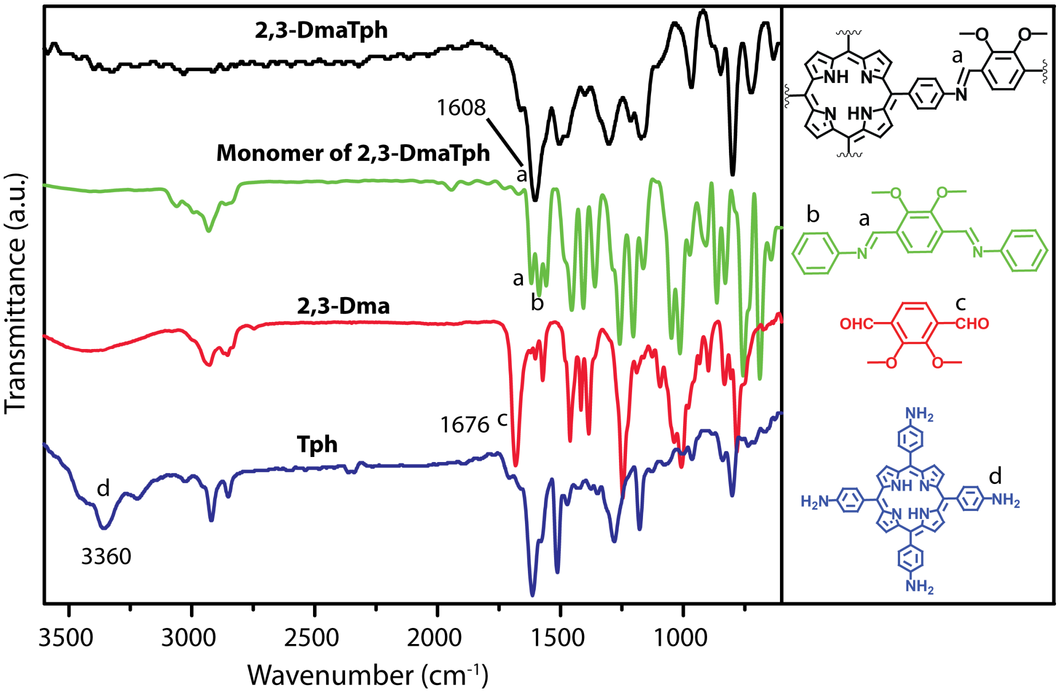

Figure S6: FT-IR spectra of **2,3-DmaTph** (Black), (*1E,1'E*)-1,1'-(2,3-dimethoxy-1,4-phenylene)bis(*N*-phenylmethanimine) (Green) (Monomer of **2,3-DmaTph**), 2,3-dimethoxyterephthalaldehyde (2,3-**Dma**) (Red), and 5,10,15,20-Tetrakis-(4-aminophenyl)-21H,23H-porphine (**Tph**) (Blue).

Section S-6: ^{13}C CP/MAS NMR Spectra of 2,3-DhaTph and 2,3-DmaTph

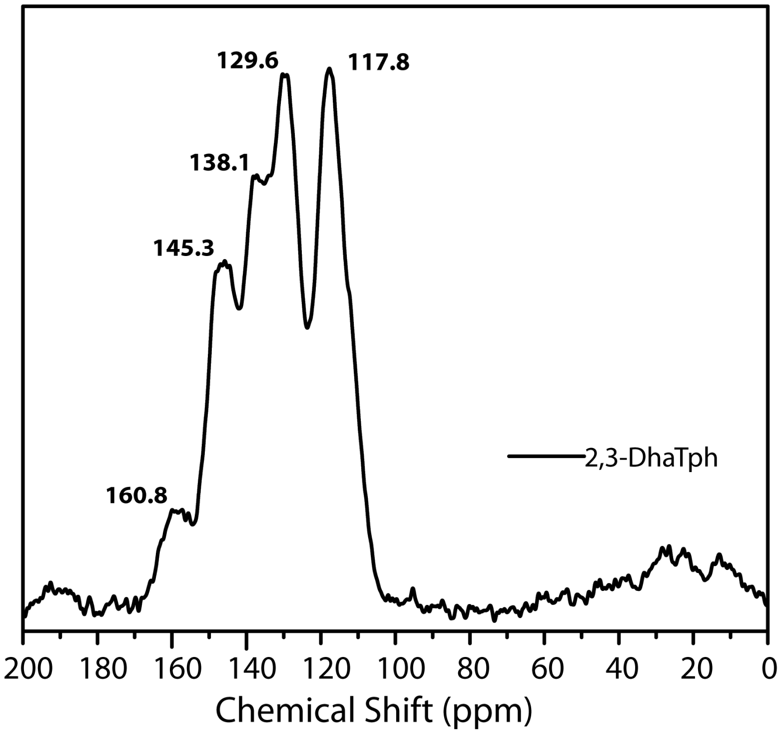

Figure S7: ^{13}C CP-MAS spectrum of **2,3-DhaTph**.

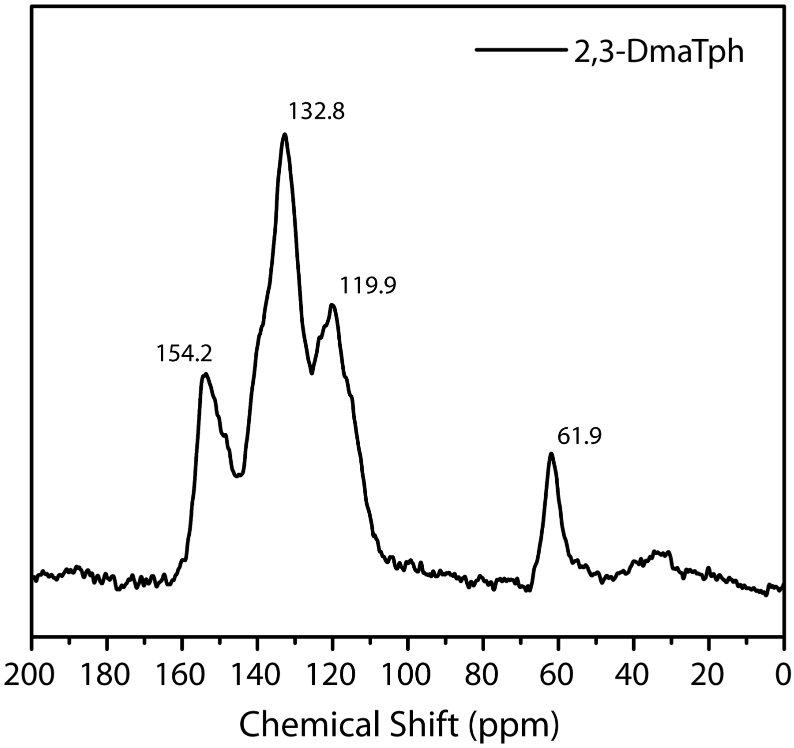

Figure S8: ^{13}C CP-MAS spectrum of **2,3-DmaTph**.

Section S-7: ^{1}H and ^{13}C NMR spectrum (Reference compound of for 2,3-DmaTph and 2,3-DhaTph)

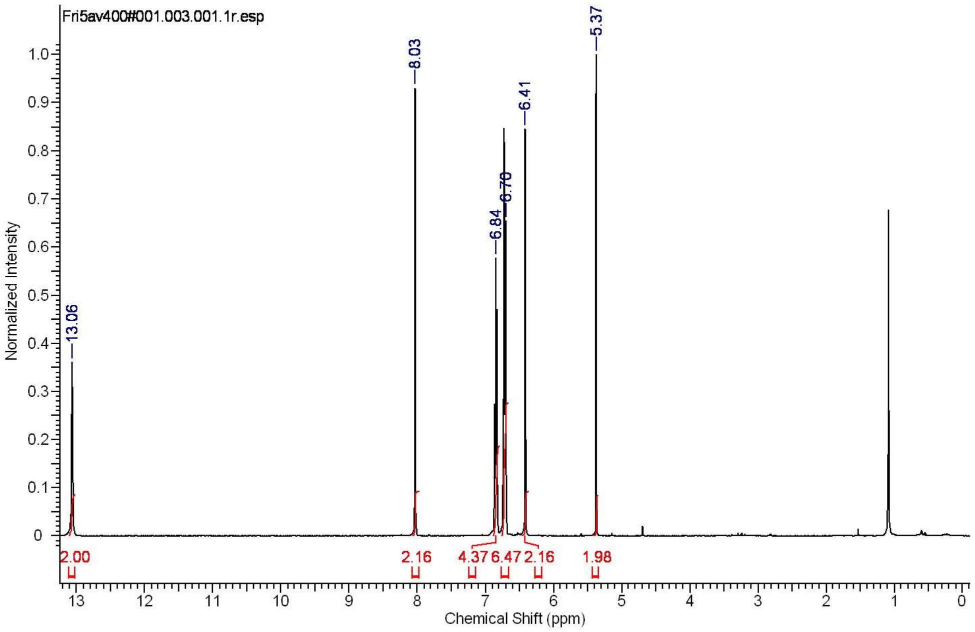

Figure S9: ^{1}H NMR 3,6-bis((*E*)-(phenylimino)methyl)benzene-1,2-diol

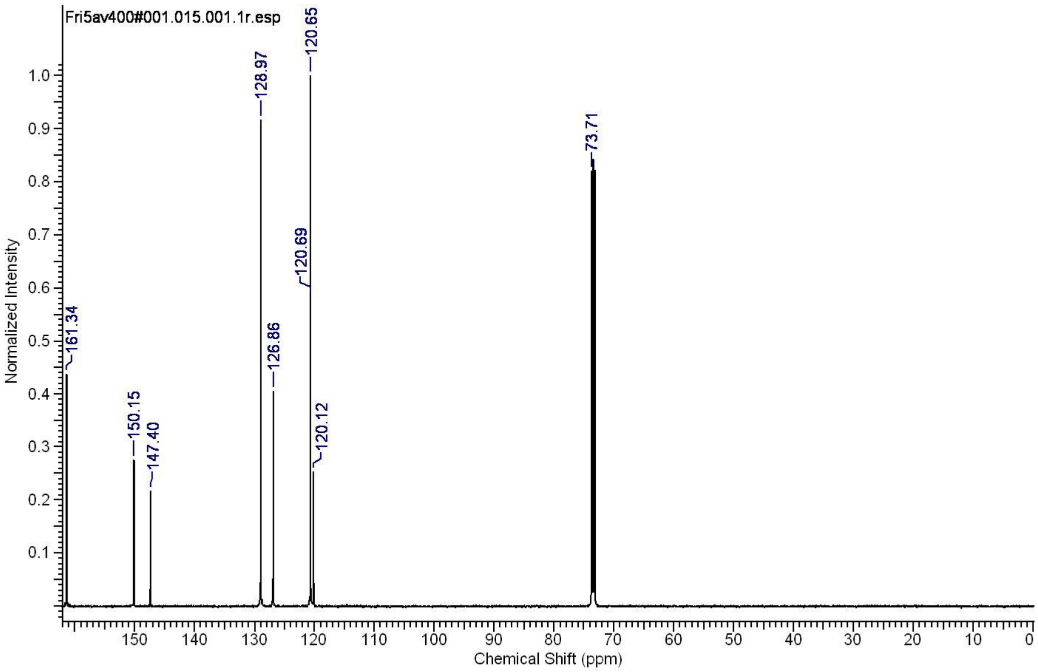

Figure S10: ^{13}C NMR of 3,6-bis((*E*)-(phenylimino)methyl)benzene-1,2-diol.

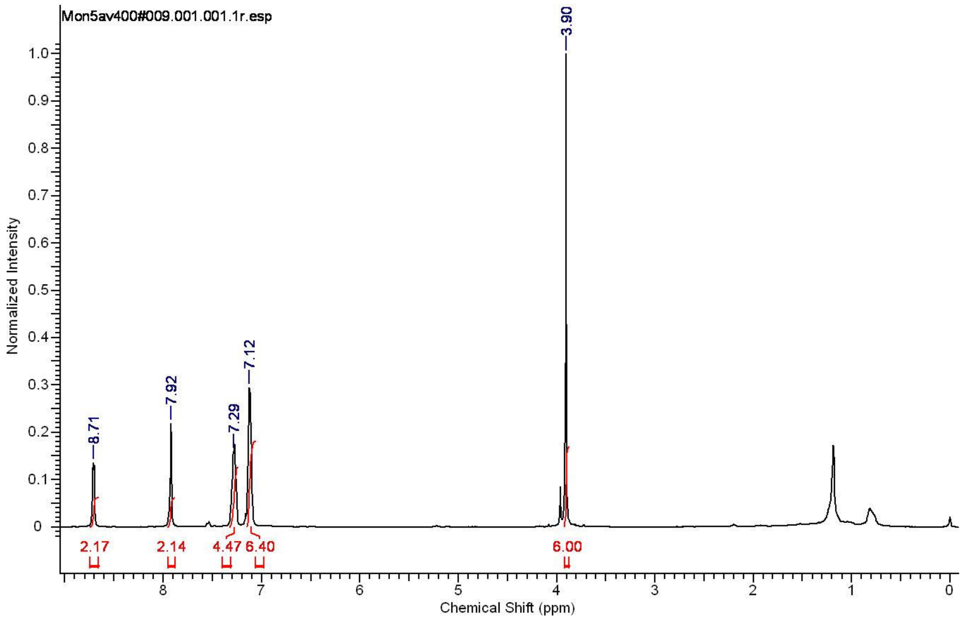

Figure S11: ^{1}H NMR of (*1E*,*1'E*)-1,1'-(2,3-dimethoxy-1,4-phenylene)bis(N-phenylmethanimine)

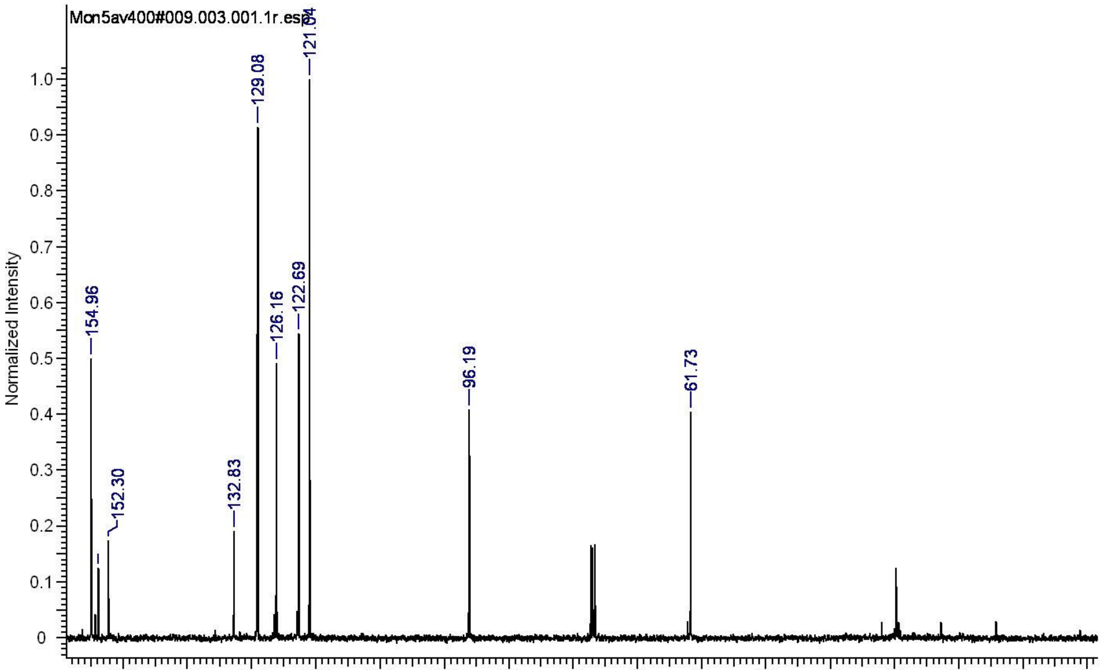

Figure S12: ^{13}C NMR of (1*E*,1'*E*)-1,1'-(2,5-dimethoxy-1,4-phenylene)bis(*N*-phenylmethanimine)

Section S-8: Gas Adsorption Studies of 2,3-DhaTph and 2,3-DmaTph

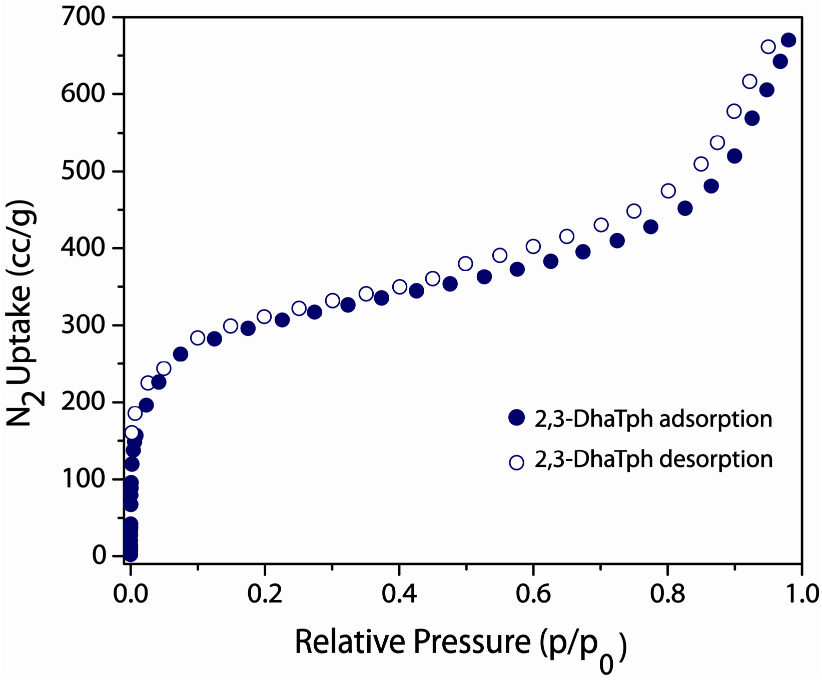

Figure S13: N_2 adsorption isotherm of **2,3-DhaTph.**

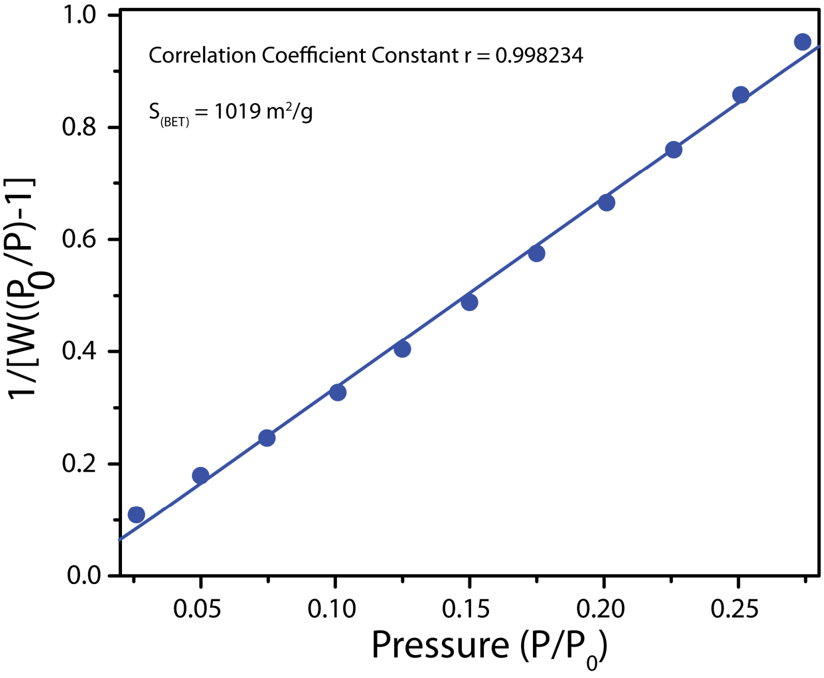

Figure S14: BET surface area plot for **2,3-DhaTph** calculated from the isotherm.

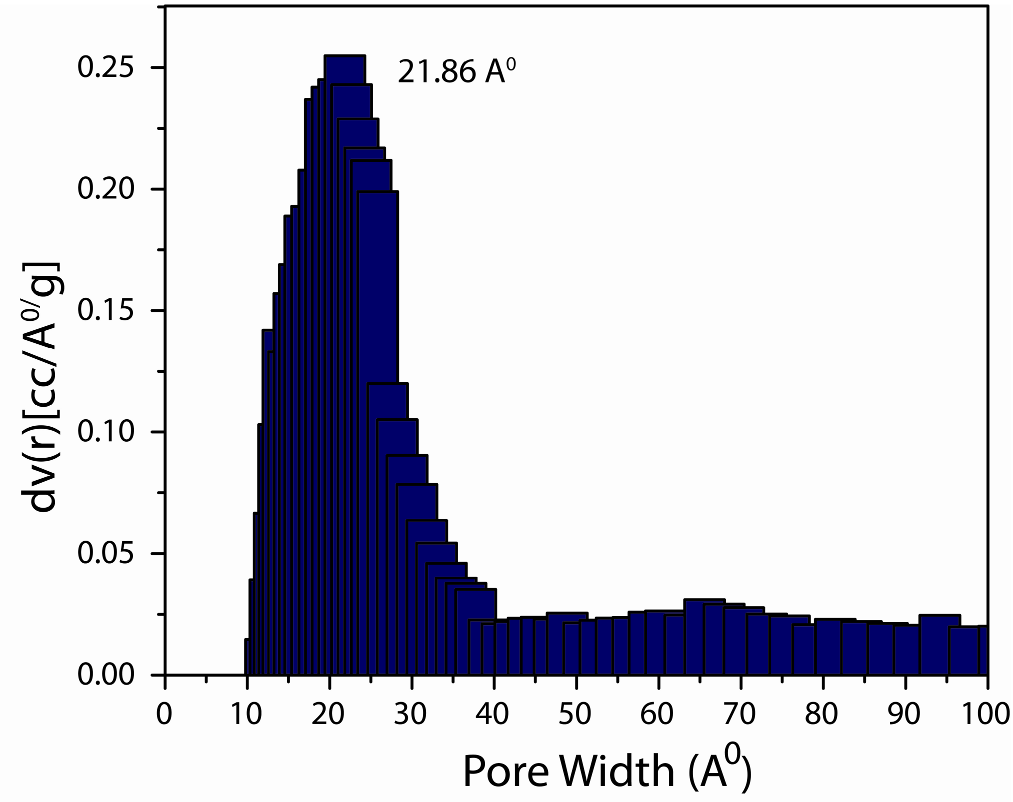

Figure S15: Pore size distribution of **2,3-DhaTph.**

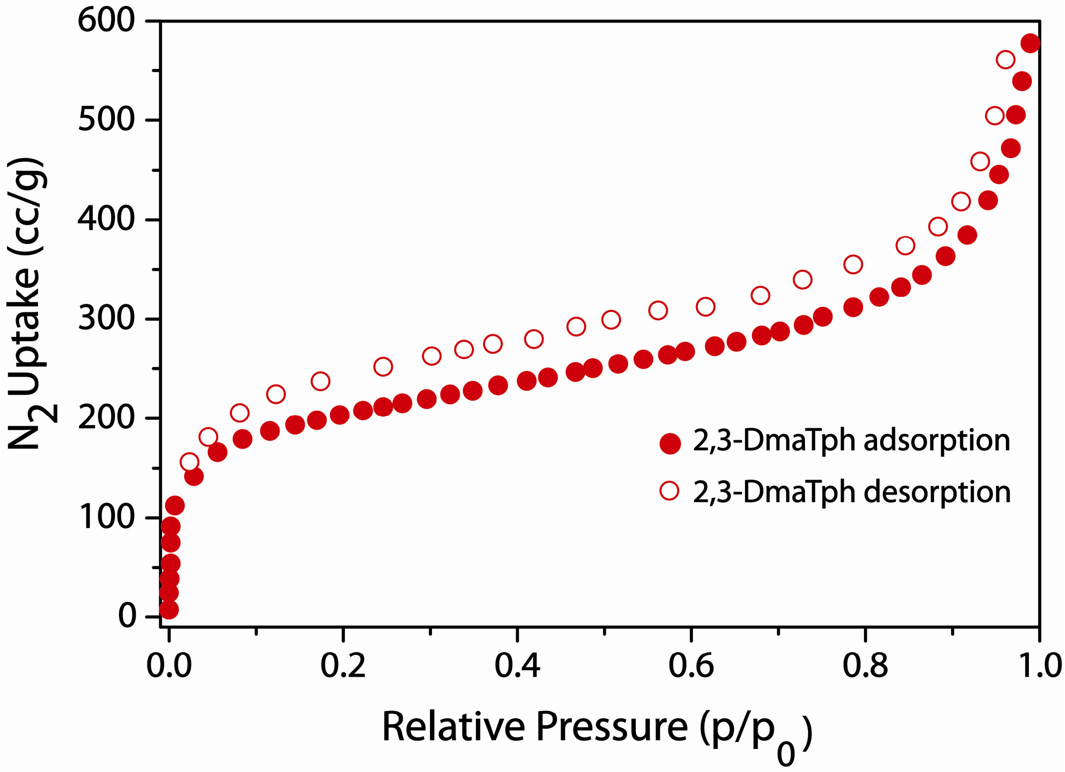

Figure S16: N_2 adsorption isotherm of **2,3-DmaTph.**

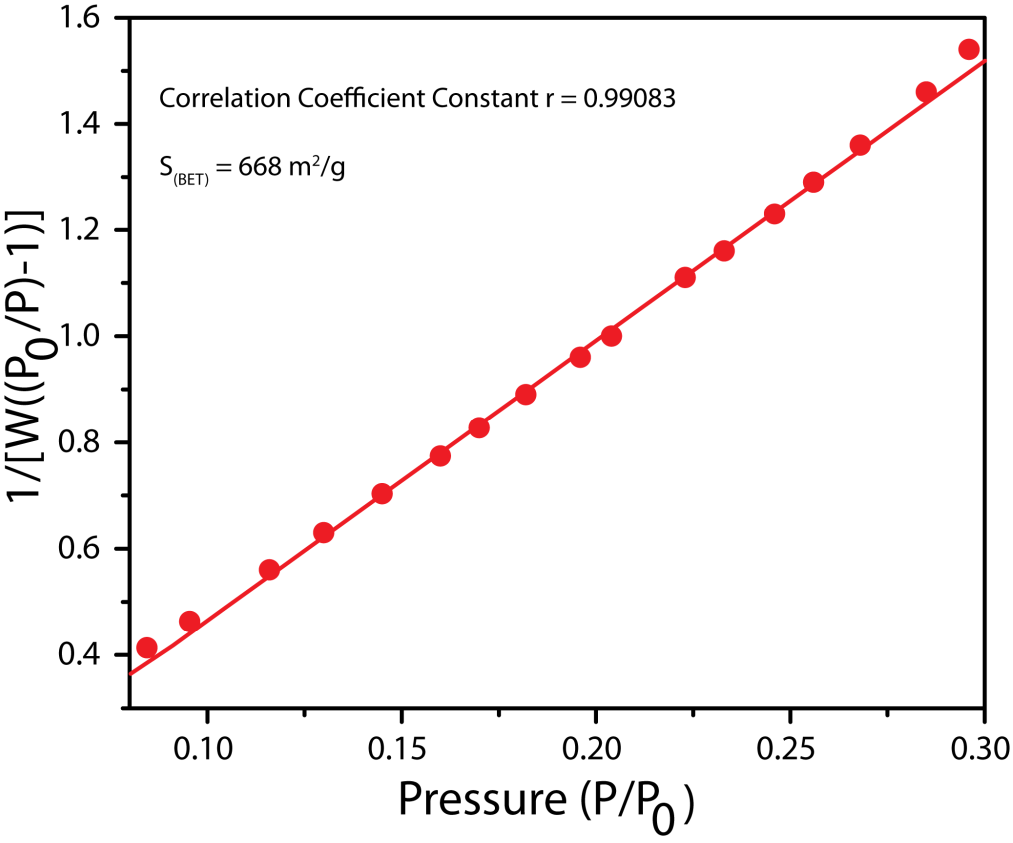

Figure S17: BET surface area plot for **2,3-DmaTph** calculated from the isotherm**.**

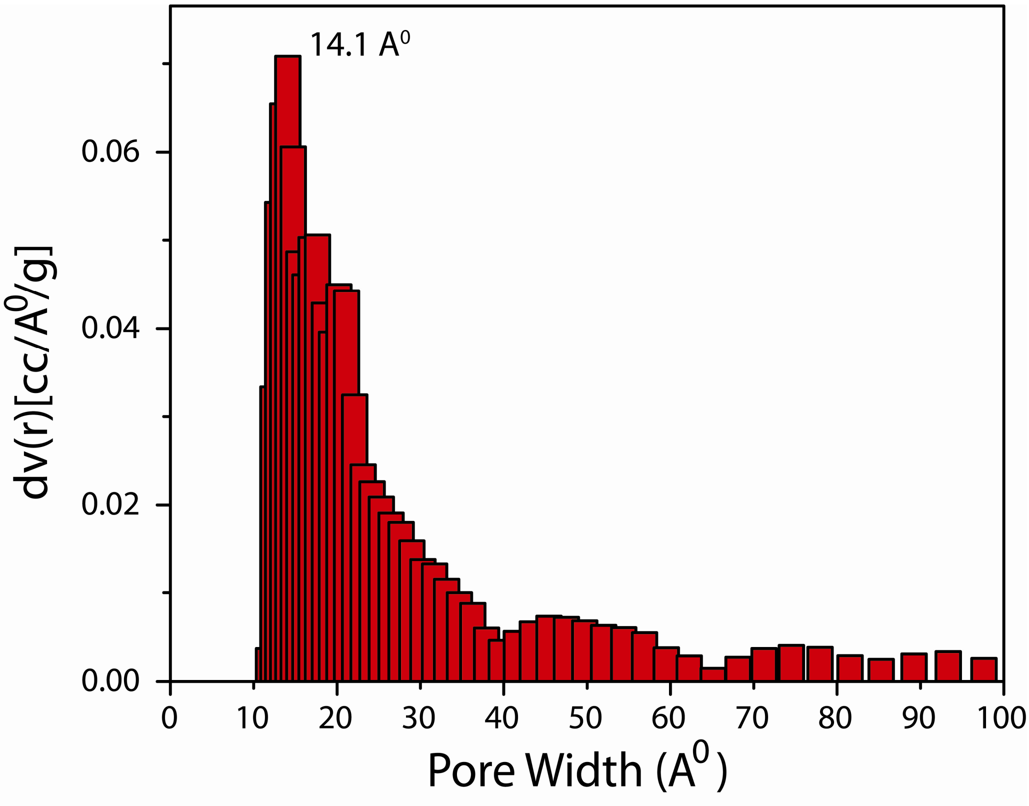

Figure S18: Pore size distribution of **2,3-DmaTph.**

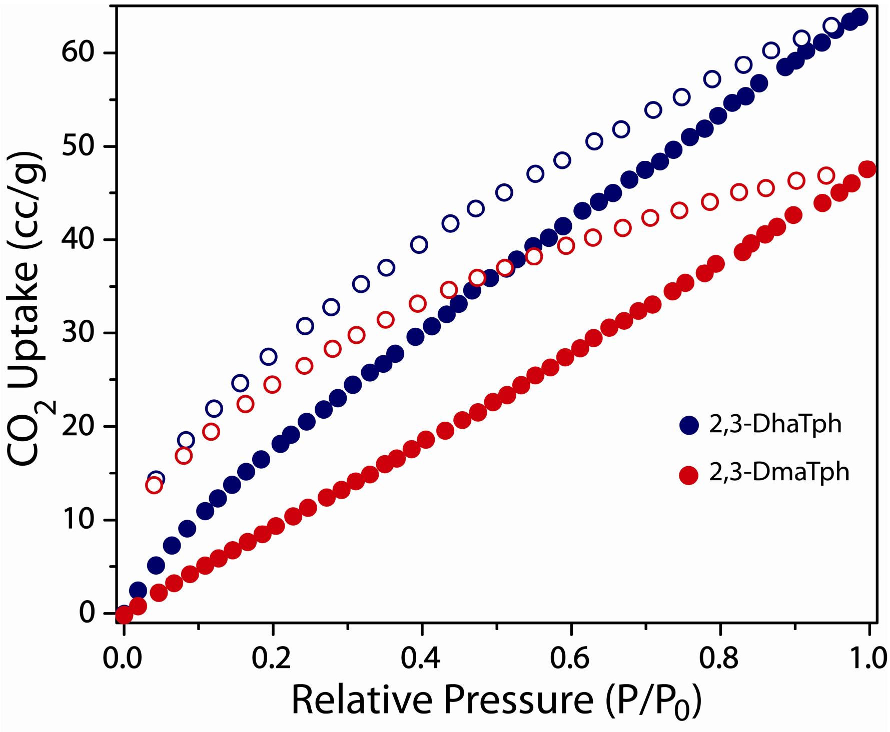

Figure S19: Carbon dioxide adsorption isotherms of **2,3-DhaTph (Blue)** and **2,3-DmaTph (Red)** at 273 K.

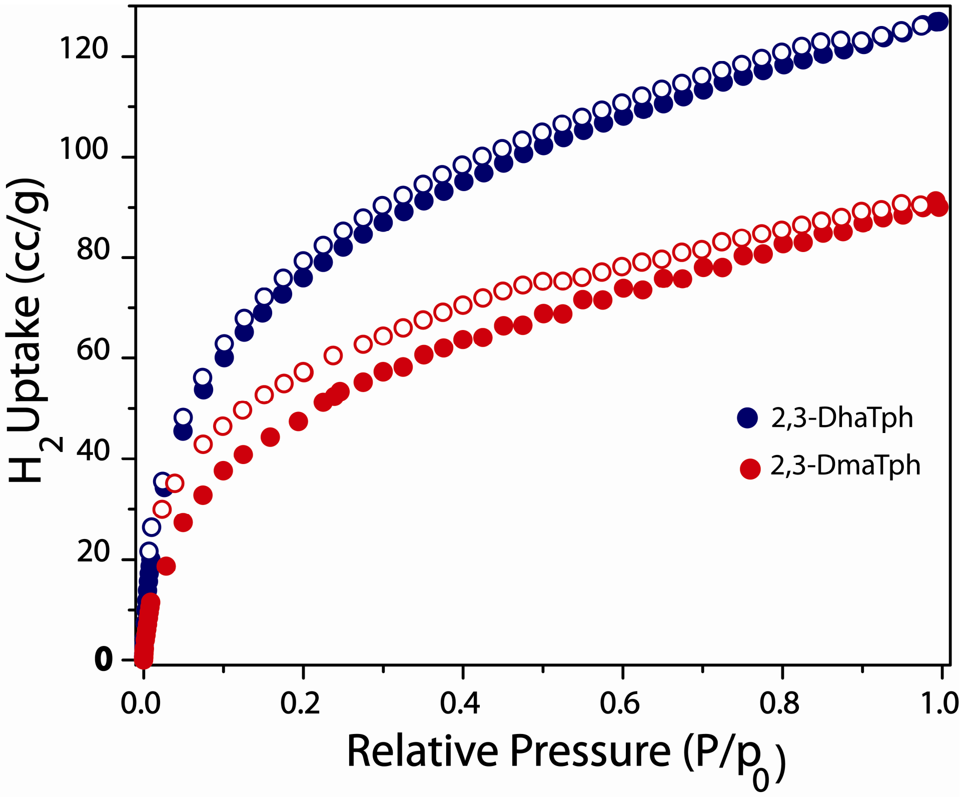

Figure S20: Hydrogen adsorption isotherms of **2,3-DhaTph (Blue)** and **2,3-DmaTph (Red)** at 77 K.

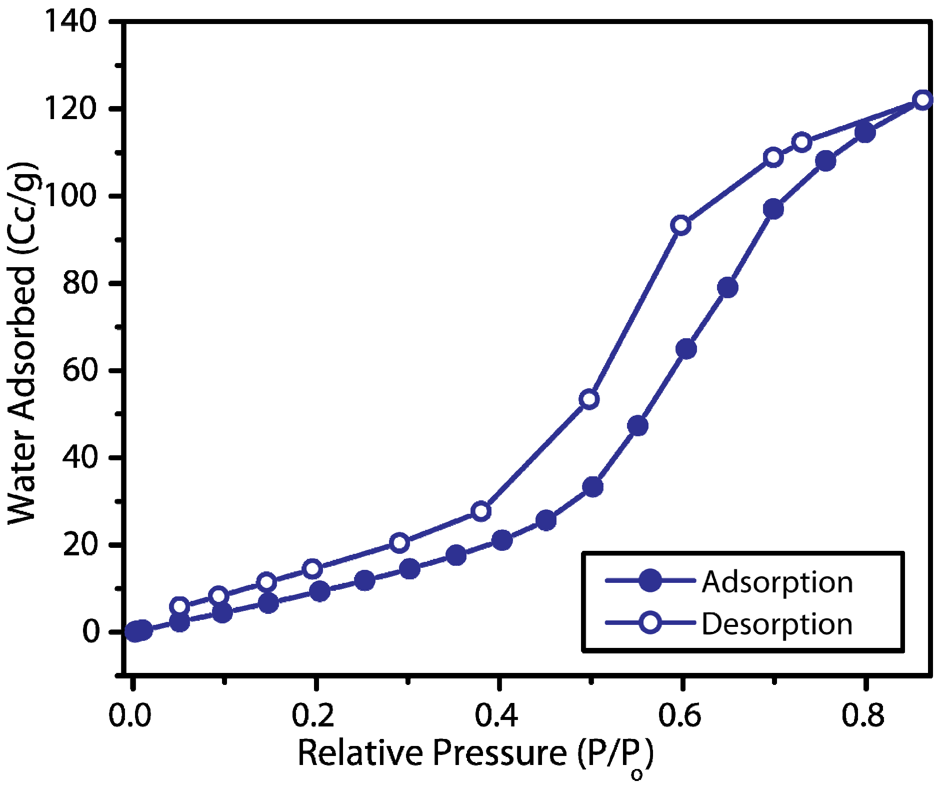

Figure S21: H_2O vapor adsorption isotherms **2,3-DhaTph**.

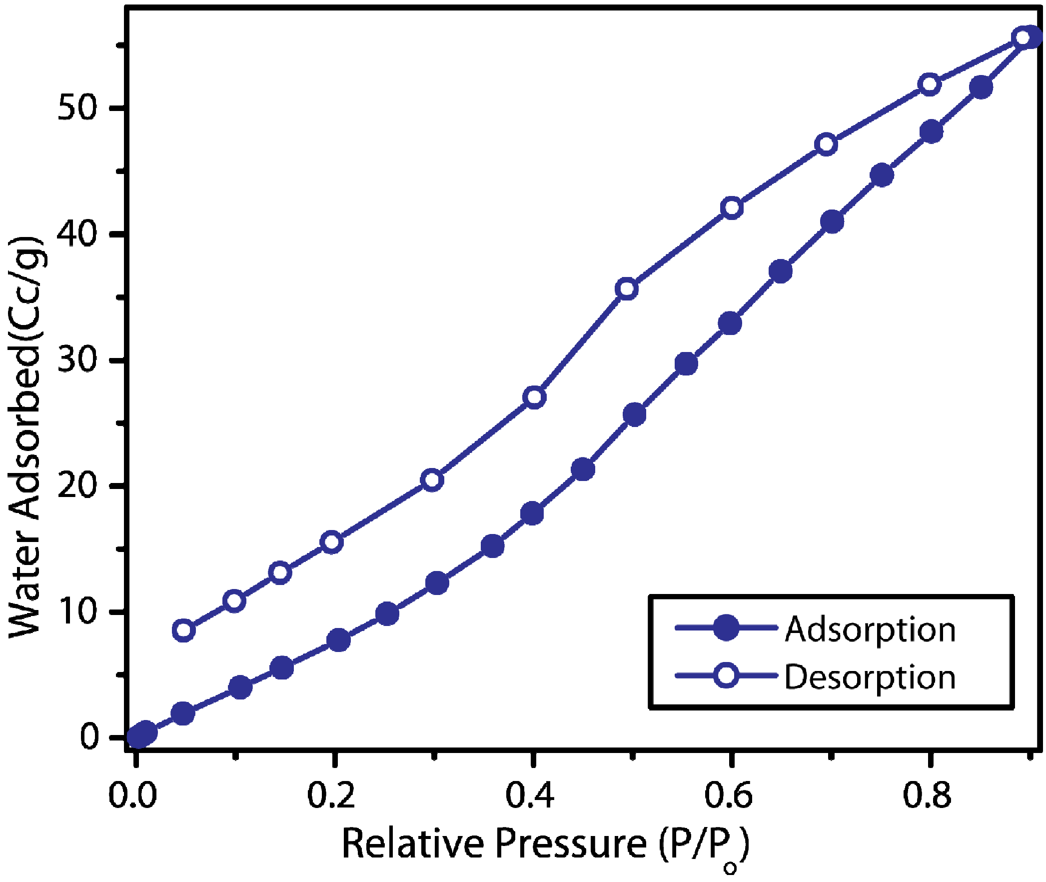

Figure S22: H_2O vapor adsorption isotherms **2,3-DmaTph**.

Section S-9:Thermogravimetric Analysis (TGA)

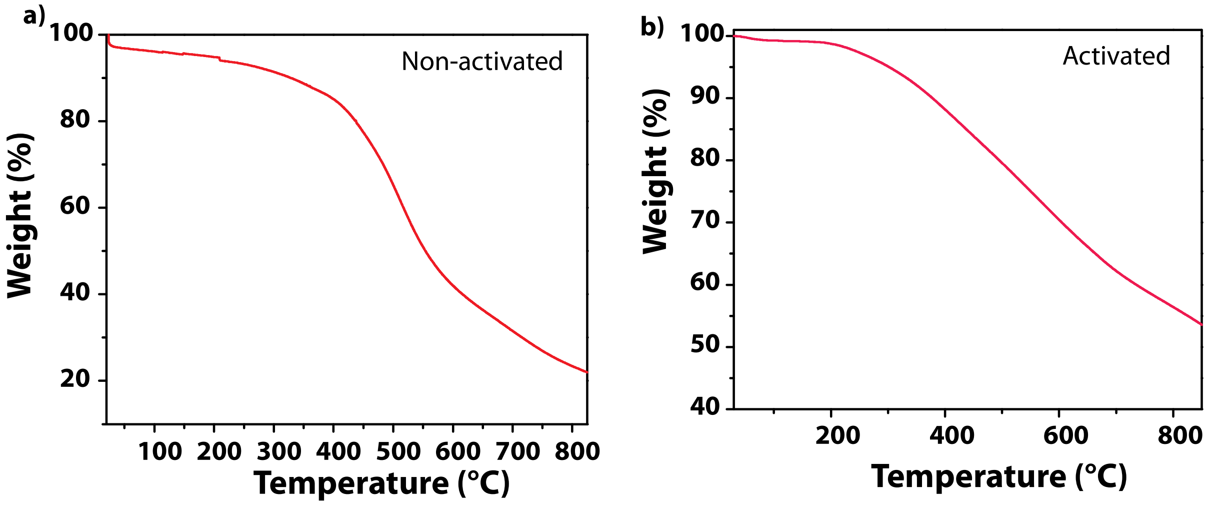

Figure S23: a) TGA data of Non-activated COF **2,3-DhaTph** under N_2 atmosphere, **b)** activated COF **2,3-DhaTph** under N_2 atmosphere.

The synthesis of COFs involves usage of very little amount of acetic acid (~100 µl). After the completion of reaction, the product was washed several times using copious amount of solvent (DMAc and EtOH) and water. Further the COF was soxleted with DMAc and activated at 150°C (under vacuum) for 12 h before subjecting it for catalysis. This stringent treatment is believed to reduce the chances of detainment of acetic acid in the material. The TGA profile of the COFs show an observable initial weight loss. However, considering the stringent washing procedures followed during the course of COF purification, acetic acid impurity seems to be unlikely present. On the other hand, the weight loss seems to be a possible result of the loss of the moisture absorbed on the COF surface. To confirm this we recorded the TGA of the activated COFs (at 150°C). Care was taken to reduce the exposure time of COF so as to decrease its ability to capture moisture. The TGA profile of the activated COF does not show observable weight loss up to 300°c. For further evidence we recorded the 13C-SSNMR of the both COFs (ESI, Section S-6). The spectra indicated the absence of peaks corresponding to the carbonyl (~ 176 ppm) and methyl (~ 23 ppm) functionalities of acetic acid, which would otherwise have appeared if acetic acid impurity was present in the COF. In the revised ESI (Section S-9) we have incorporated freshly collected TGA Data

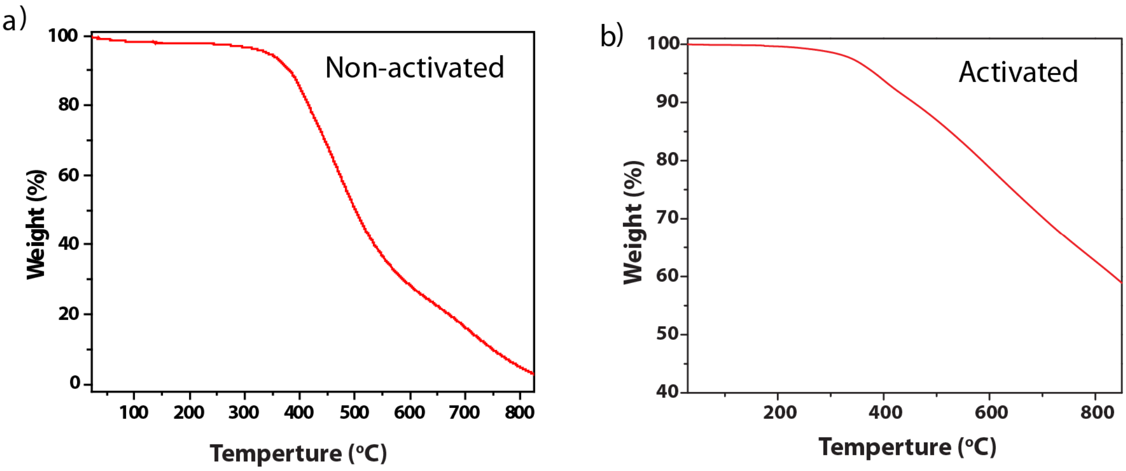

Figure S24: a) TGA data of Non-activated COF **2,3-DmaTph** under N_2 atmosphere, **b)** activated COF **2,3-DmaTph** under N_2 atmosphere.

Note: Non-activated means the COF sample which was recovered by filteration and simple drying , which shows wieght loss of ~ 80-90 % due to the oligomeric impurity in the material. But the **Activated** sample means the COF which was isolated and well washed with organic solvents (DMAc and ethanol) and water, further the COF material was activated at 150 °C (under vacuum) for 12 hours, which shows weight loss of ~ 45-50 %.

Section S-10: Scanning Electron Micrographs (SEM) and Transmission Electron Micrographs (TEM)

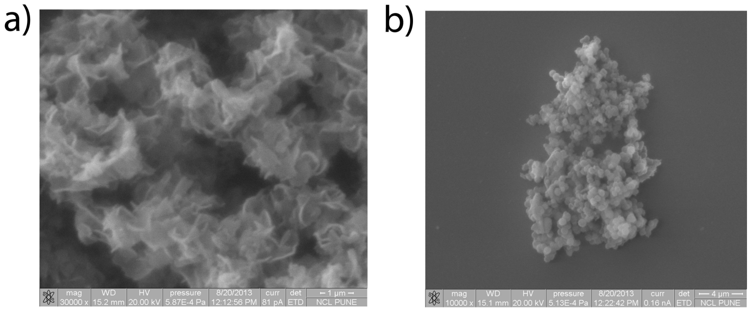

Figure S25: SEM images of **a) 2,3-DhaTph** and **b) 2,3-DmaTph.**

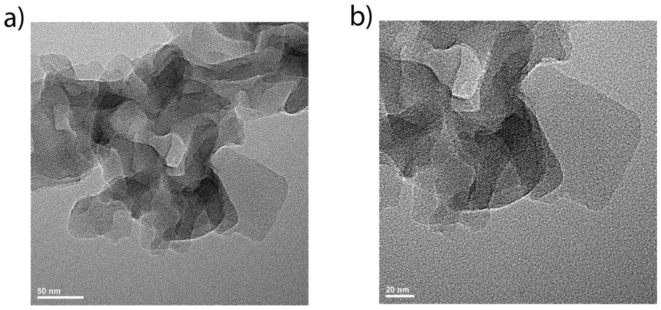

Figure S26: TEM images of **2,3-DhaTph.**

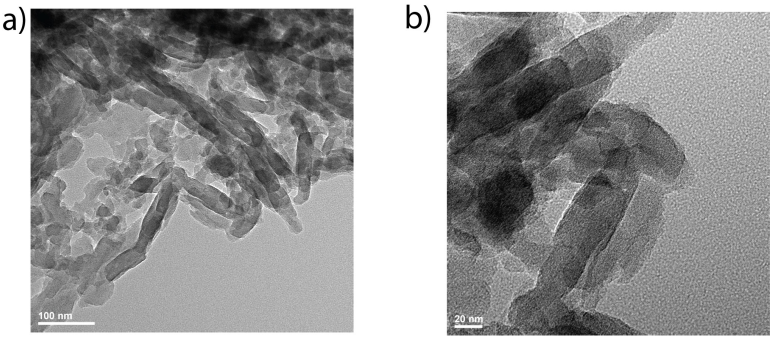

Figure S27: TEM images of **2,3-DmaTph**.

Section S-11: X-Ray investigation of single crystals of linker-2,3-DhaTph and 2,3-DmaTph

Moiety formula $C_{20}H_{16}N_2O_2$, space group- $P\ 4_3\ 2_1\ 2$, a = 7.0094(3) Å, b = 7.0094(3) Å, c = 32.787(2) Å, α = 90°, β = 90°, γ = 90°, V = 1610.88 (17) $Å^3$, Z = 4, Dx = 1.304, 4166 reflections measured, 1889 unique reflections, R = 0.0588, Rw = 0.1455.

Cambridge Crystallographic Data Centre identifier:CCDC 1019814

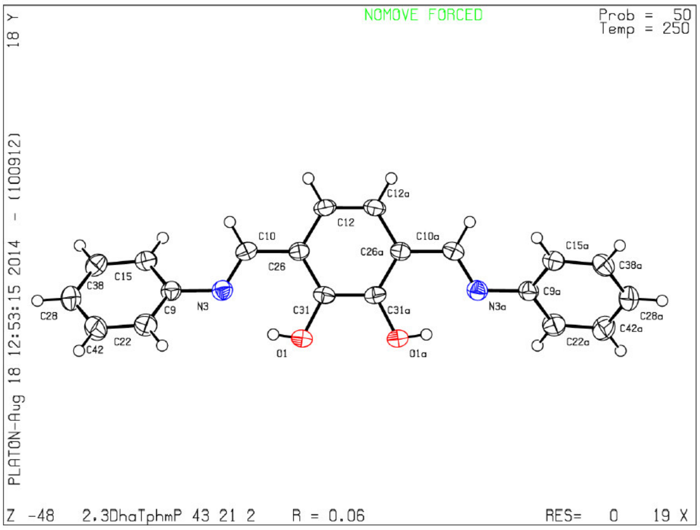

Figure S28: ORTEP diagram of 2,5-bis((E)-(phenylimino)methyl)benzene-1,4-diol with thermal ellipsoids at 50% probability**.**

Moiety formula $C_{22}H_{20}N_2O_2$, space group- P b c n, a= 15.715(3) Å, b= 12.1408(14) Å, c= 9.9342(12) Å, α = 90°, β = 90°, γ = 90°, V = 1895.4(5) $Å^3$, Z = 4, Dx = 1.207, 7652 reflections measured, 2527 unique reflections, R = 0.0883, Rw = 0.3453.

Cambridge Crystallographic Data Centre identifier:CCDC 1019813

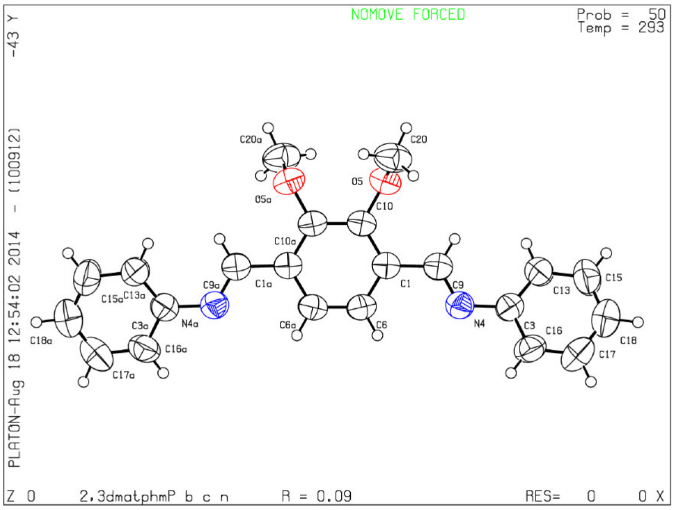

Figure S29: ORTEP diagram of (*1E,1'E*)-1,1'-(2,5-dimethoxy-1,4-phenylene)bis(*N*-phenylmethanimine) with thermal ellipsoids at 50% probability.

Section S-12: Stability test for 2,3-DhaTph

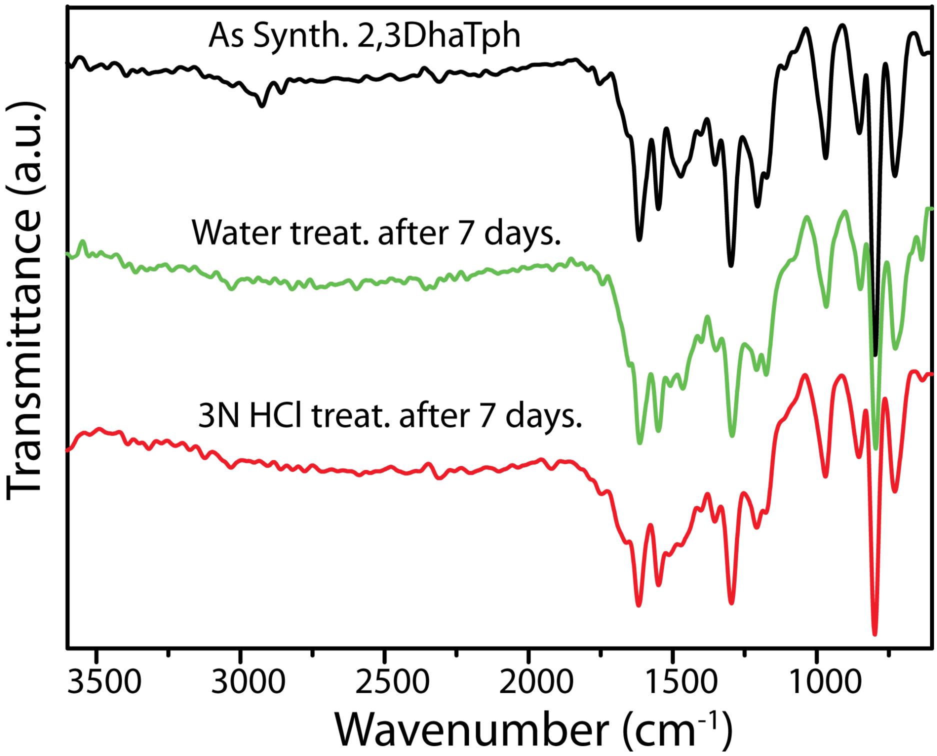

Figure S30: IR of **2,3-DhaTph** after treatment with water, and acid after 7 days.

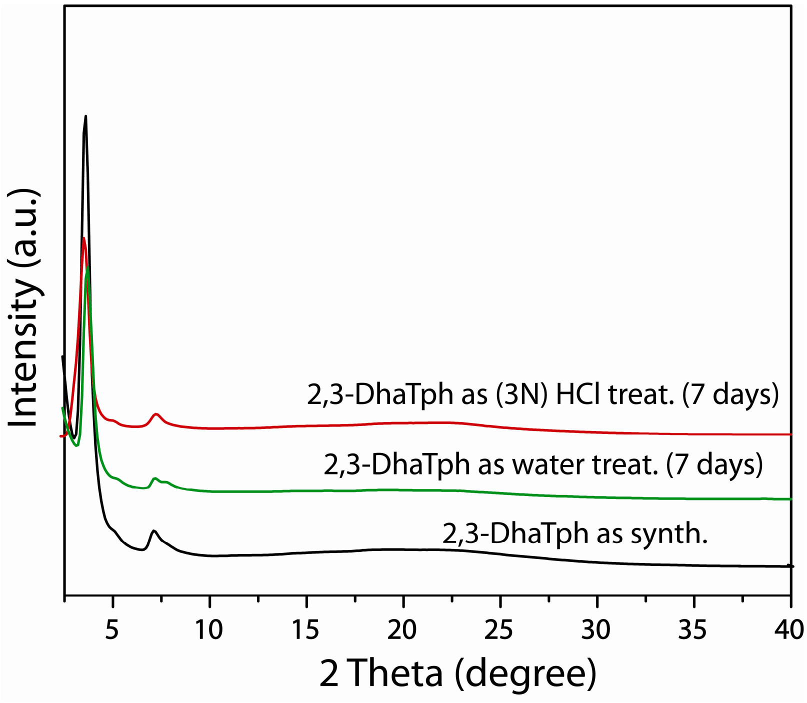

Figure S31: PXRD of **2,3-DhaTph** after treatment with water and acid for 7 days.

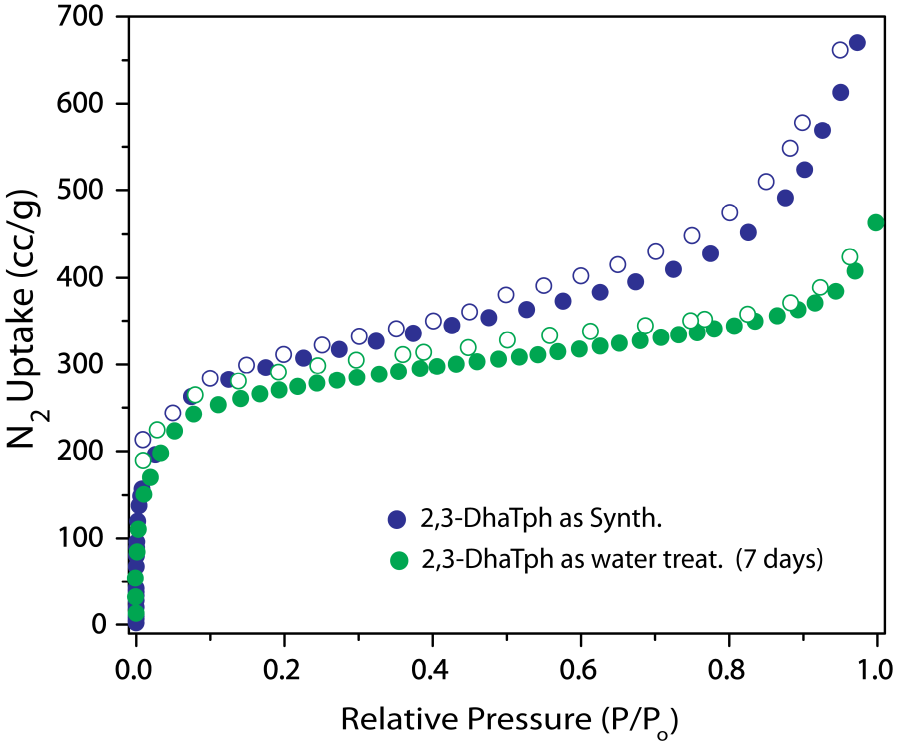

Figure S32: N_2 Uptake of **2,3-DhaTph** after treatment with water for 7 days.

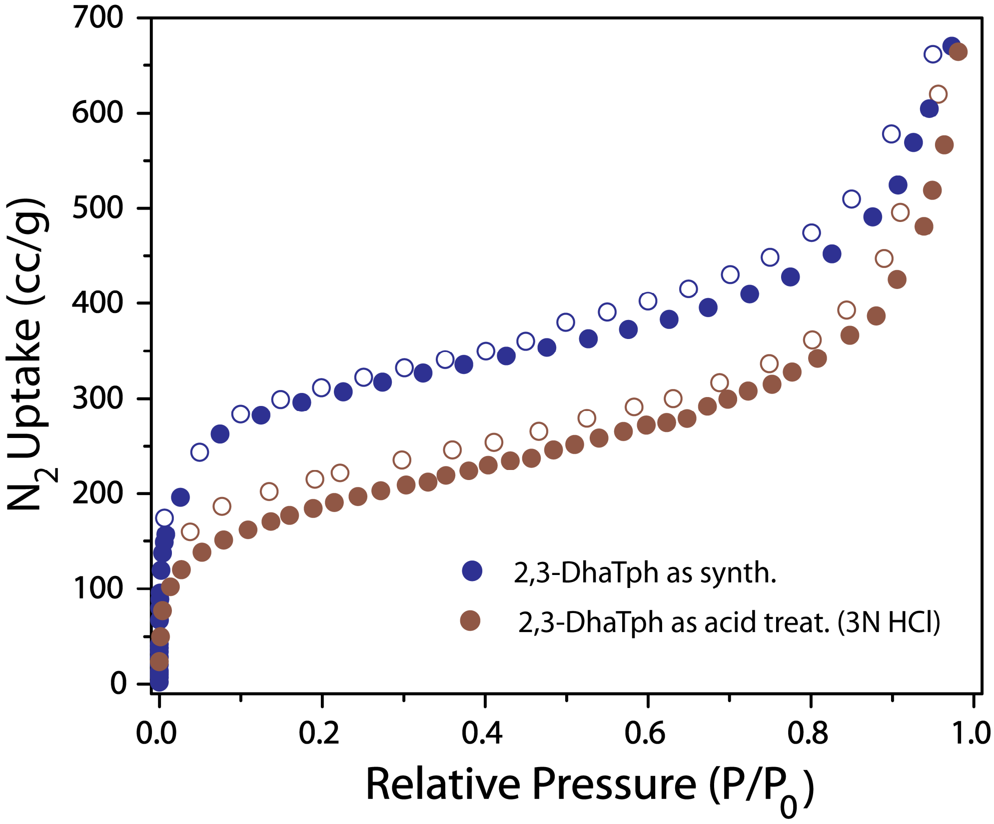

Figure S33: N_2 Uptake of **2,3-DhaTph** after treatment with 3N HCl for 7 days.

Stability test for 2,3-DmaTph

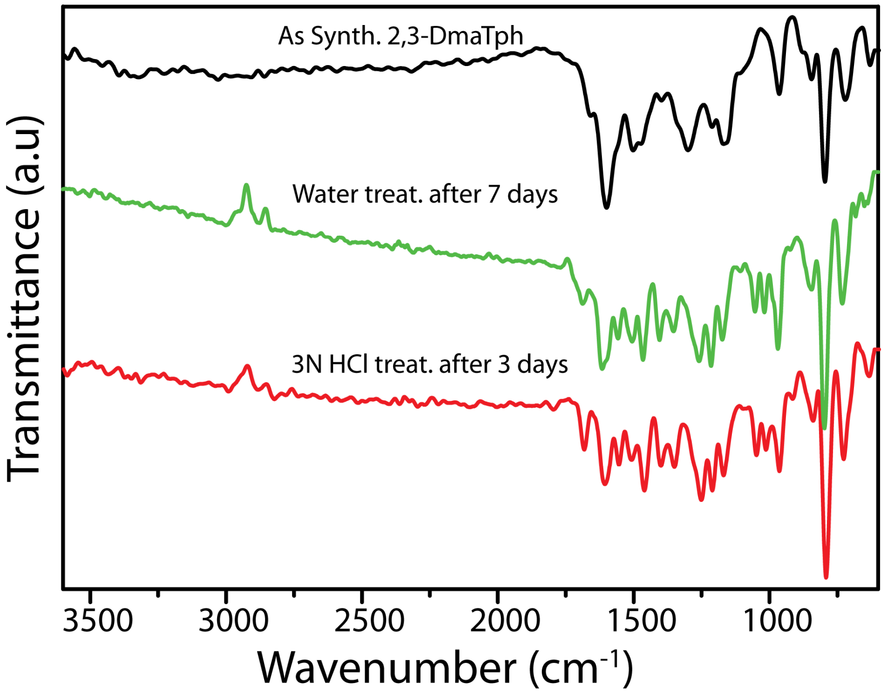

Figure S34: IR of **2,3-DmaTph** after treatment with water for 7 days and acid for 3 days.

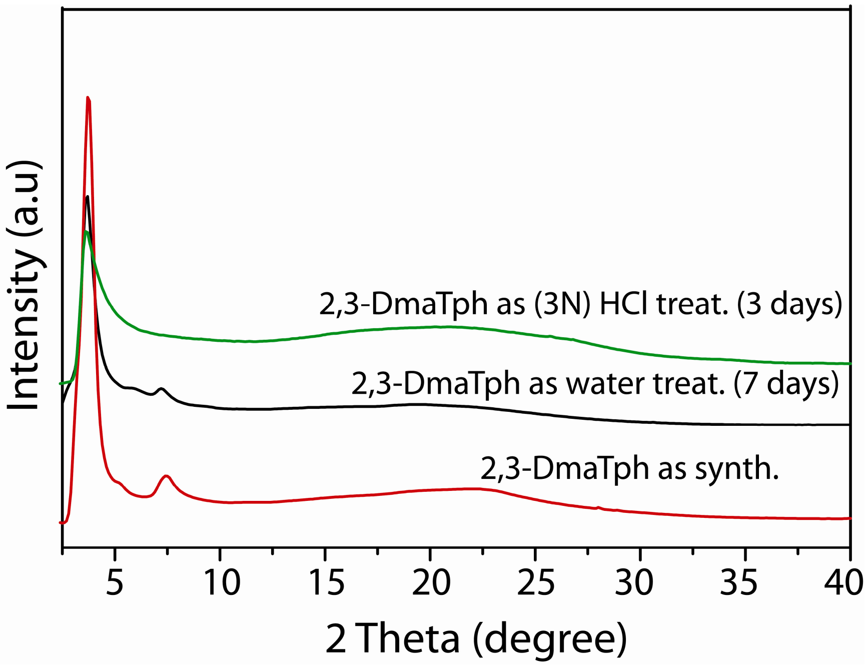

Figure S35: PXRD of **2,3-DmaTph** after treatment with water for 7 days and acid for 3 days.

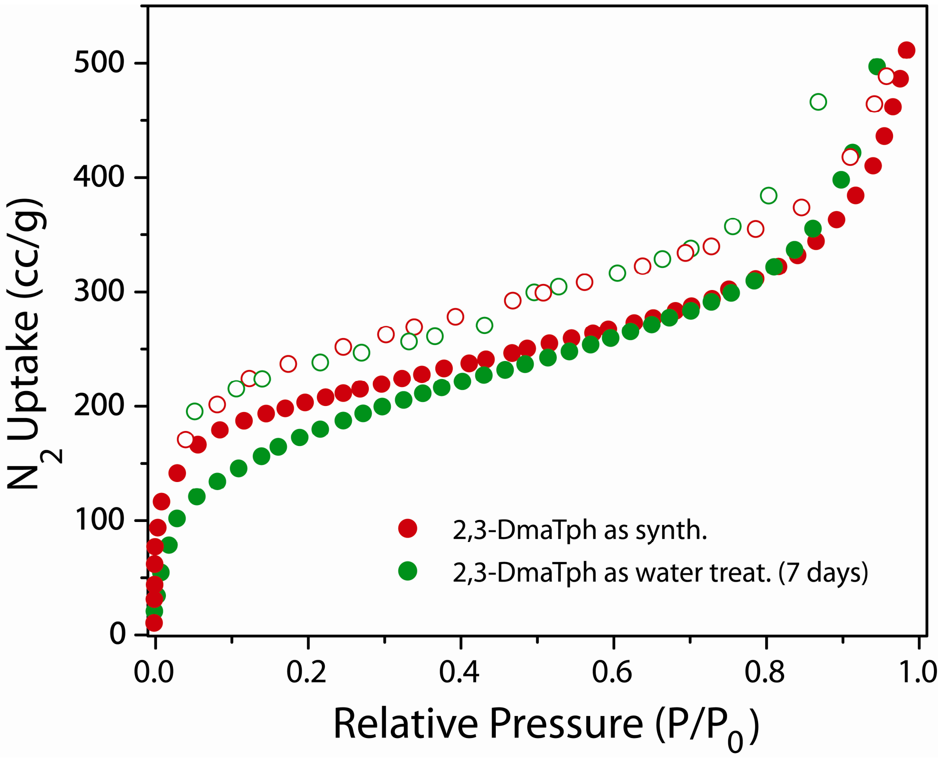

Figure S36: N_2 Uptake of **2,3-DmaTph** after treatment with water for 7 days.

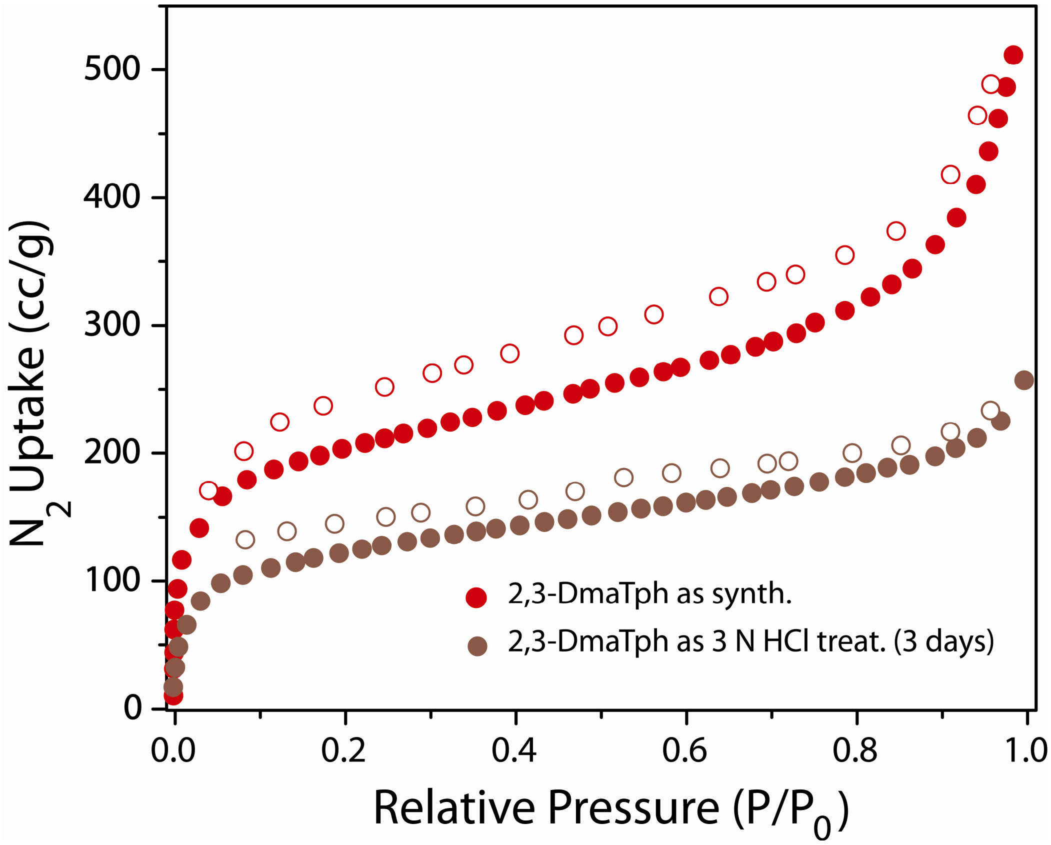

Figure S37: N_2 Uptake of **2,3-DmaTph** after treatment with 3N HCl for3 days.

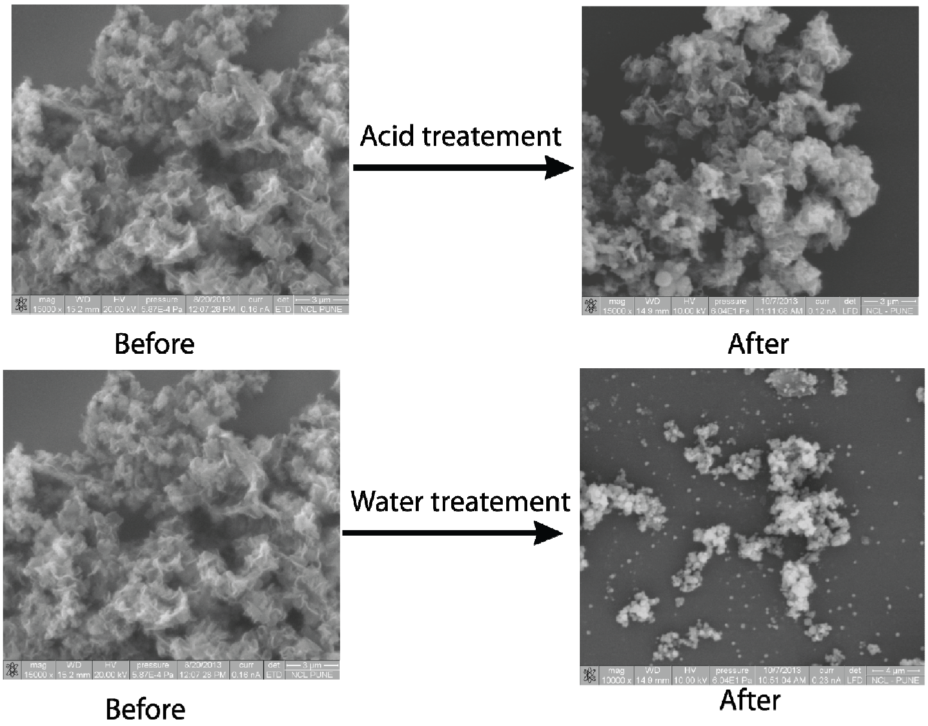

Figure S38: SEM images of **2,3- DhaTph** before and after acid treatment.

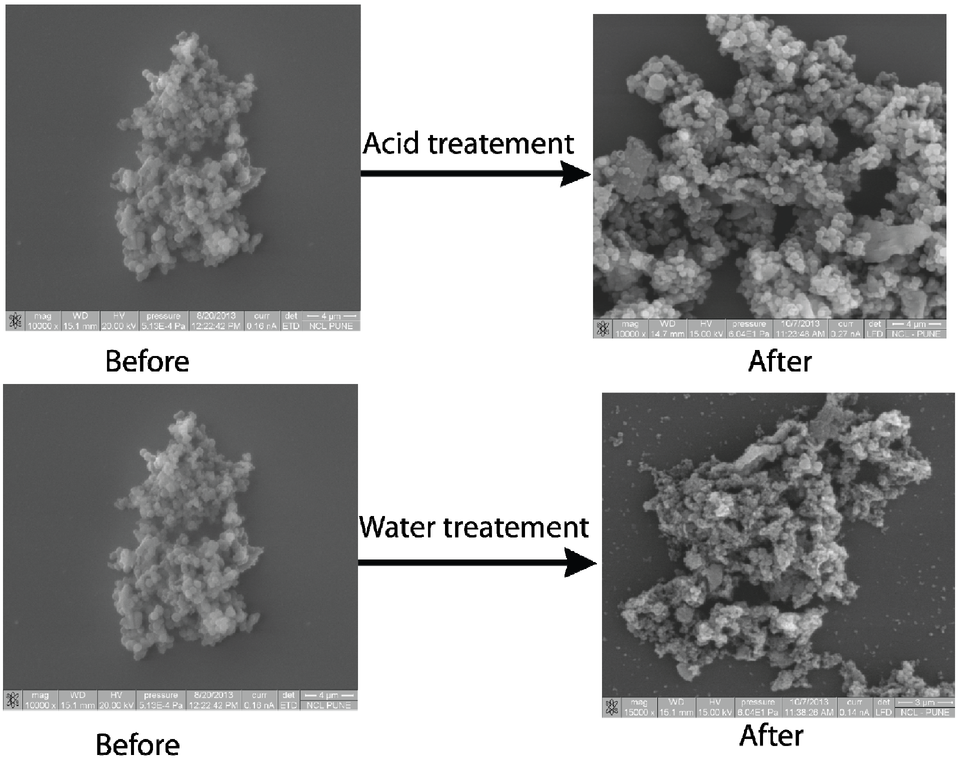

Figure S39: SEM images of **2,3-DmaTph** before and after acid treatment.

Section S-13: Before and after Catalyst (2,3-DhaTph and 2,3-DmaTph)

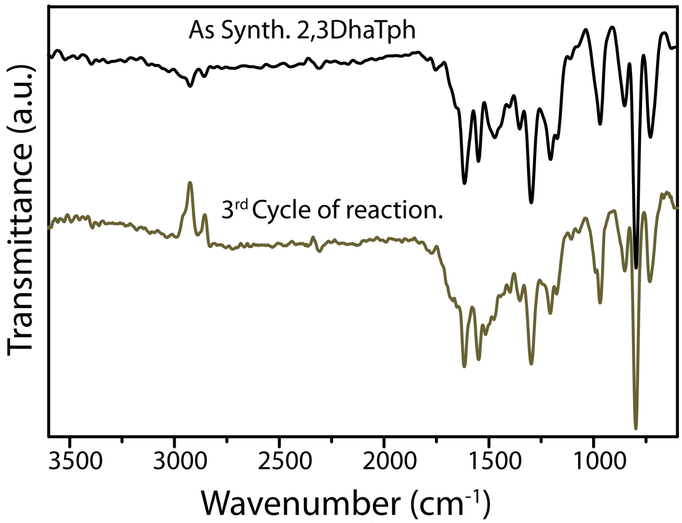

Figure S40: IR of **2,3-DhaTph** after reaction (3rd Cycle)

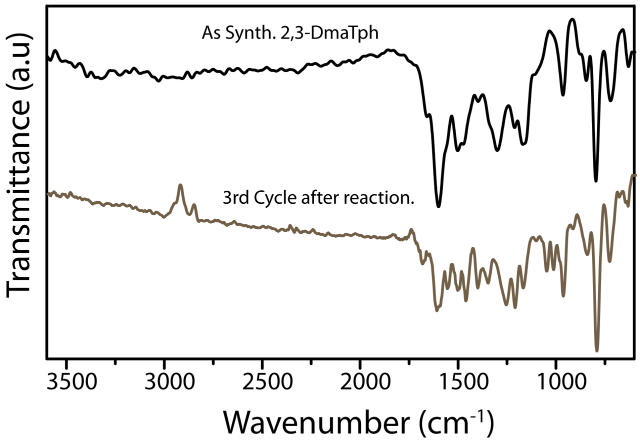

Figure S41: IR of **2,3-DmaTph** after reaction (3^{rd} Cycle)

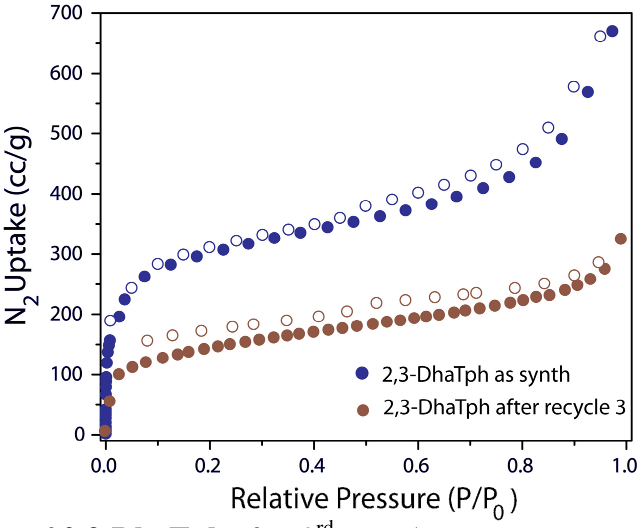

Figure S42: N_2 Uptake of **2,3-DhaTph** after 3^{rd} recycle.

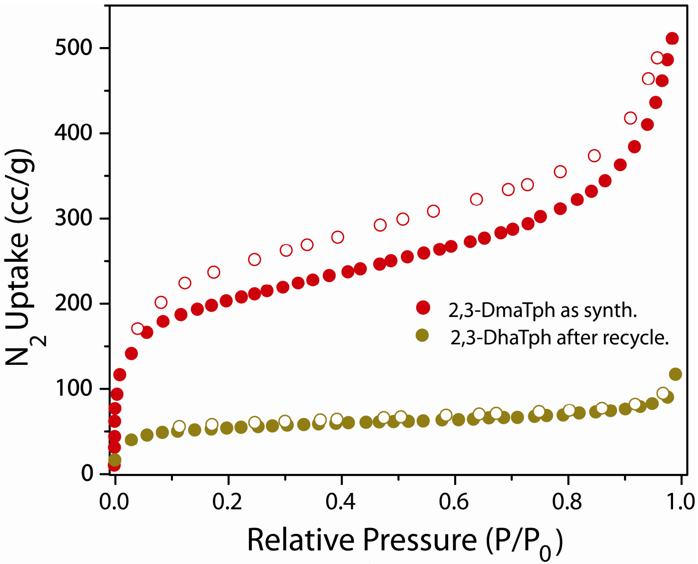

Figure S43: N_2 Uptake of **2,3-DmaTph** after 3^{rd} recycle.

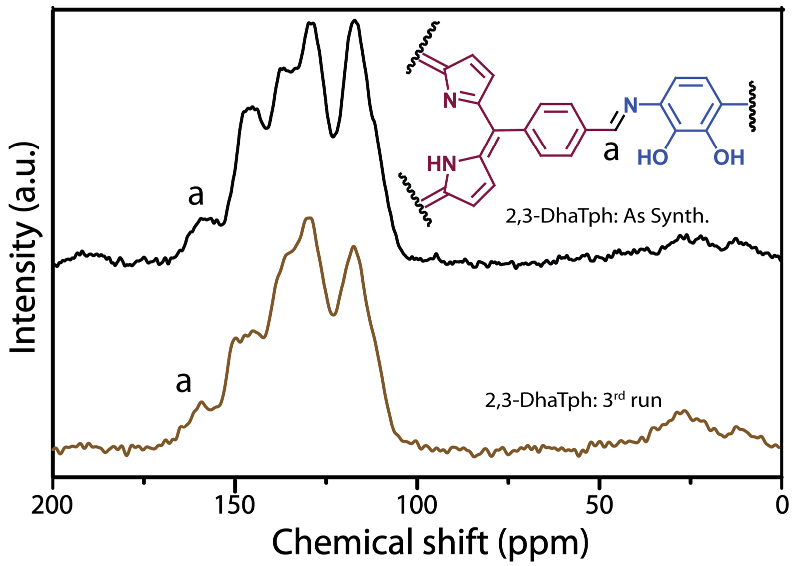

Figure S44: SSNMR of **2,3-DhaTph** after 3rd recycle.

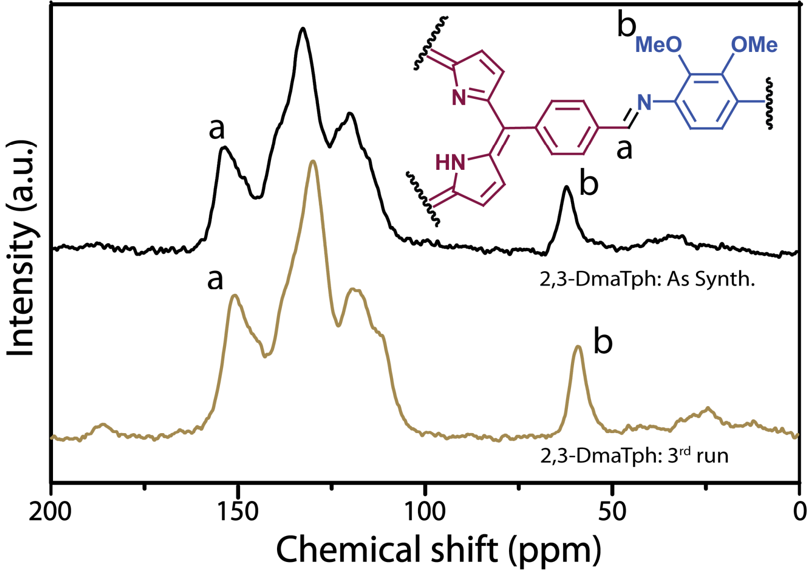

Figure S45: SSNMR of **2,3-DmaTph** after 3rd recycle.

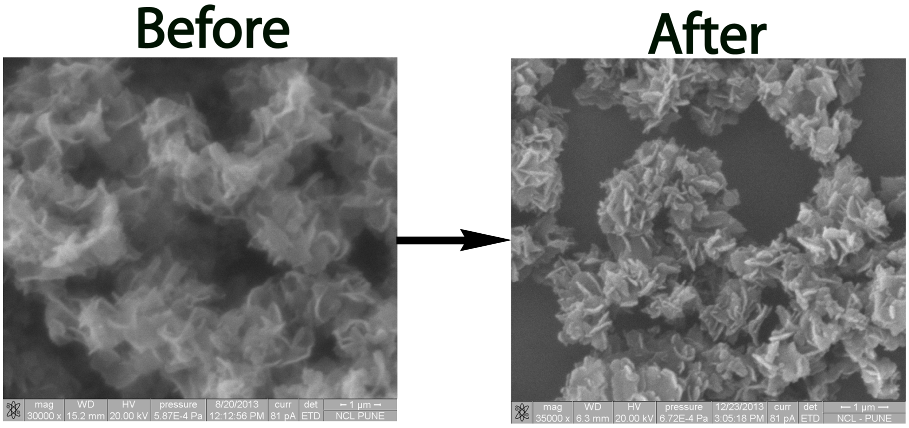

Figure S46: SEM images of **2,3-DhaTph** before and after reaction.

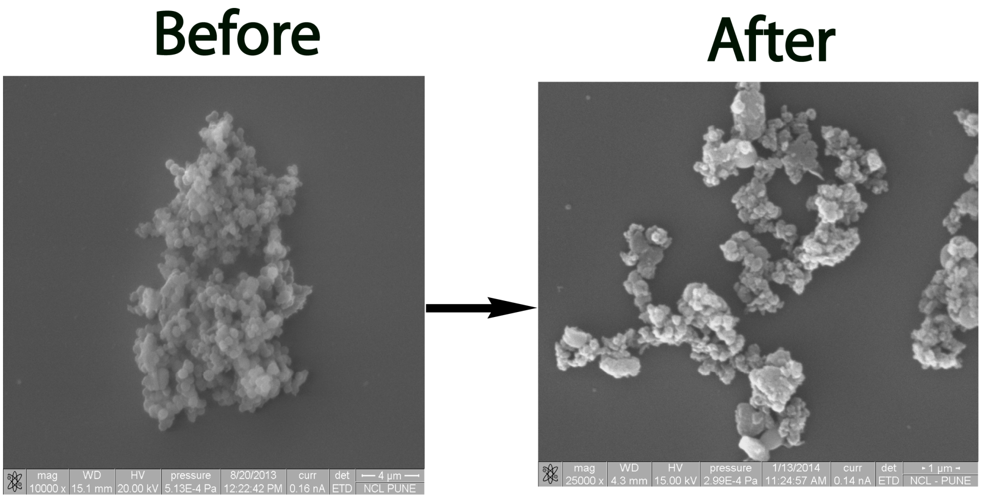

Figure S47: SEM images of **2,3-DmaTph** before and after reaction.

Section S-14: Optimiozation of catalyst

Table 3: Bifunctional COF as catalyst for cascade recation.

Entry	Catalyst	Conversion (%)	Yield (%) GC	
			2	3
1	Blank	32	27	5
2	2,3-DhaTph	100	4	96
3	2,3-DmaTph	54	2	52
4	DhaTph	99	5	94

Table 4: Cascade reaction catalyzed by 2,3-DhaTph and 2,3-DmaTph

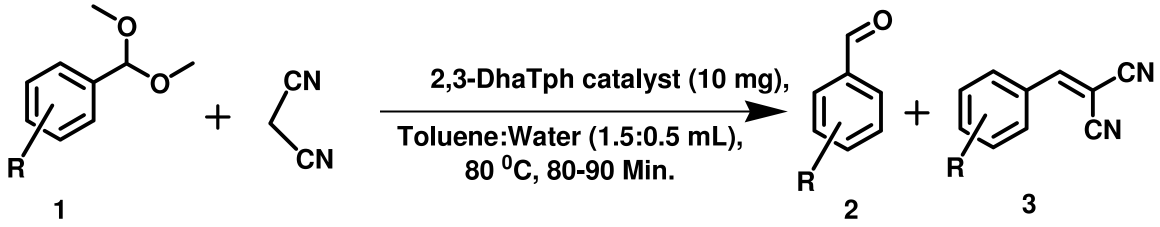

Entry	Acetal (1)	Product (2)	Product (3)	Time (min)	Catalyst	Yield (%)
1	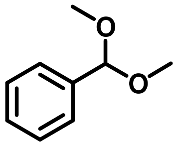	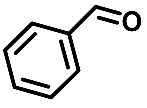	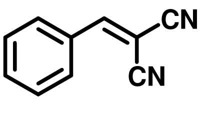	85	**2,3-DhaTph**	96
					2,3-DmaTph	52

2	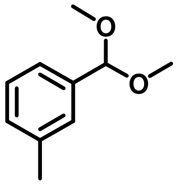	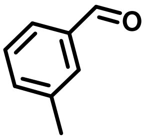	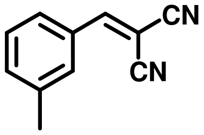	90	**2,3-DhaTph**	85
					2,3-DmaTph	46
3	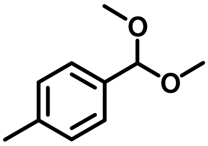	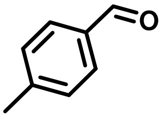	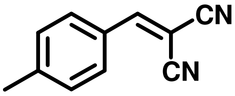	85	**2,3-DhaTph**	90
					2,3-DmaTph	50
4	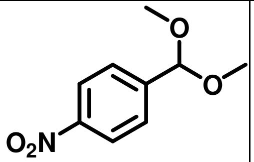	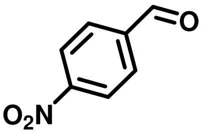	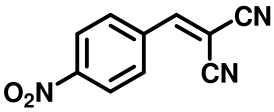	90	**2,3-DhaTph**	82
					2,3-DmaTph	40
5	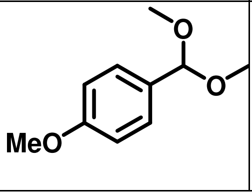	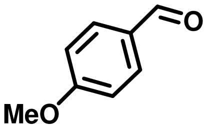	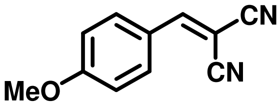	85	**2,3-DhaTph**	86
					2,3-DmaTph	48

Charcterization of Product (3)[4]:

2-(Phenylmethylene)malononitrile (3a):

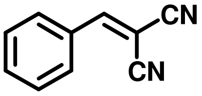

^{1}HNMR (200 MHz, CDCl$_3$): δ 7.95 (2H, d, *J* = 7.5 Hz,), 7.81 (1H, s,), 7.59 (1H, t, *J* = 7.3 Hz,), 7.50-7.48 (2H, m).

2-(3-Methylphenylmethylene)malononitrile (3b):

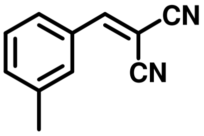

^{1}H-NMR (200MHz, CDCl$_3$): δ 7.70 (2H, d, 2H, J = 6.2 Hz), 7.64 (1H, s), 7.36 (1H, s), 7.41 (1H, t, J = 7.3 Hz), 2.44 (3H, s).

2-(4-Methylphenylmethylene)malononitrile (3c):

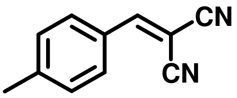

^{1}H NMR (200 MHz, CDCl$_3$): δ 7.84 (2H, d, *J* = 7.8 Hz,), 7.31 (2H, d, *J* = 7.8 Hz,), 7.18 (1H, s,), 2.38 (3H, s).

2-[(4-Nitrophenyl)methylene]malononitrile (3d):

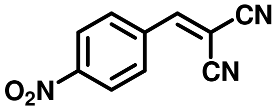

^{1}HNMR (200 MHz, $CDCl_3$): δ 8.1 (2H, d, *J* = 8.2 Hz), 7.7 (1H, s), 7.5 (2H, d, *J* = 8.4 Hz).

2-[(4-Methoxyphenyl)methylene]malononitrile (3e):

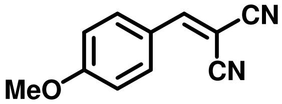

^{1}HNMR (200 MHz, $CDCl_3$): δ 7.9 (2H, d, *J* = 8.0 Hz), 7.6 (1H, s), 7.0 (2H, d, *J* = 8.0 Hz), 3.9 (3H, s).

Section S-15: References

1) K. Grudzień, M. Malinska, M. Barbasiewicz, *Organometallics* **2012,** *31*, 3636.

2) B. Lukose, A. Kuc, T. Heine, *Chem. Eur. J.* **2011**, *17*, 2388.

3) Accelrys, Material Studio Release Notes, Release 4.2, Accelrys Software, San Diego **2006**.

4) G. R. Krishnan, K. Sreekumar, *Eur. J. Org. Chem.* **2008**, 4763.